MASTER IN BIOMEDICINE PROFESSIONAL FOCUS

Study of the Heterodimerization of ABCB5β with ABCB6 and ABCB9 using NanoBRET Assay

Gerard, Louise

Award date:
2019

Awarding institution:
University of Namur

Faculté de Médecine

STUDY OF THE HETERODIMERIZATION OF ABCB5β WITH ABCB6 AND ABCB9 USING NANOBRET ASSAY

Mémoire présenté pour l'obtention

du grade académique de master en sciences biomédicales

Louise GERARD

Janvier 2018

Université de Namur
FACULTE DE MEDECINE
Secrétariat des départements
Rue de Bruxelles 61 - 5000 NAMUR
Téléphone: + 32(0)81.72.43.22
E-mail: manon.chatillon@unamur.be - http://www.unamur.be/

Study of the Heterodimerization of ABCB5β with ABCB6 and ABCB9 Using NanoBRET Assay

GERARD Louise

Abstract

ATP Binding Cassette (ABC) transporters are primary active transporters. They transport a wide range of substrates (e.g. ions, peptides, amino acids, sugar, xenobiotics, etc.) and use the energy from ATP hydrolysis to translocate molecules across membranes against their chemical gradient. They play a major role in drug pharmacokinetics and cancer multidrug resistance. A body of evidence support the role of several ABC transporters in tumorigenesis. ABCB5, a member of the ABCB family also known as multidrug resistance (MDR) family, can be found, among other cellular types, in melanocytes in the basal layer of epidermis. ABCB5 plays a specific role in melanoma chemoresistance and tumor cells progression. There are several isoforms including ABCB5 full length, ABCB5*β*, ABCB5*α* and others small transcripts. This study focuses on the "half like" transporter ABCB5*β* and more precisely on its potential heterodimerization with other half-transporters of the B family. The ABCB5*β* heterodimerization with ABCB6 and ABCB9 was evaluated given the common points between theses transporters. ABCB5*β* and ABCB6 are both upregulated in melanoma, involved in multidrug resistance and related to some diseases such as *dyschromatosis universalis hereditaria*. ABCB9 and ABCB5*β* show a similar localization profile in testis. To determine whether these half transporters dimerize, the Nano Bioluminescence Resonance Energy Transfer (NanoBRET) method has been performed. The study revealed that ABCB5β heterodimerizes with ABCB6 and ABCB9. Furthermore, data also indicate that ABCB6 and ABCB9 can dimerize. This work shed some light on the biology of ABCB5, a little characterized ABC transporter.

Keywords: ABCB family, ABCB5β, protein-protein interaction, dimerization, NanoBRET.

Mémoire de master en sciences biomédicales

Janvier 2019

Thesis Supervisor: Jean-Pierre Gillet

Acknowledgments

I would like to thank Professor Gillet for his fosterling in his laboratory and his encouragement, advice and correction.

I would like to give a special thank you to Laurent Duvivier for his patience and implication in my master thesis. It was a pleasure working with you, you were more sympathetic than Manuel! Thank you to Marie, Emilie, Miguel, Florence, Géraldine and Camille for the great time in the office and all the help given. Thanks to the UrPhym members for their advices and welcoming. Thanks to Professor Le Tallec for his help in the statistic part.

Thanks to my housemates and friends Théo, Jean-Benoit, Phanio, Luigi, Julien and Antoine for their support at any time of the day and night. Thank you to my friend and family without whom these five years would have never finished. Thank you to Céline, Emilie and my parents for everything they have done and all the time spent for me.

A very special thanks to Eleonore, your advice and support mean a lot. What a well followed plan! Finally, for you Thibaut, your encouragements were essential and you would have been the first to congratulate me if you were still here.

Table of content

Abbreviation

ABC: ATP Binding Cassette

ABCB5 FL: ABCB5 Full-Length

ACT: Adoptive Cell Therapy

ASR: Age Standardized Mortality

ATP: Adenosine Triphosphate

CSD: Chronic Sun Induced

DNA: Deoxyribonucleic Acid

DHFRPCA: Dihydrofolate Reductase Protein-Fragment Complementation Assay

EMT: Epithelial Mesenchymal Transition

FRET: Forster Resonance Energy Transfer

GFP: Green Fluorescent Protein

HEK: Human Embryonic Kidney

MDR: Multidrug Resistance

NanoBRET: Nano Bioluminescence Resonance Energy Transfer

NBD: Nucleotide Binding Domain

PCA: Protein-fragment Complementation Assay

PCR: Polymerase Chain Reaction

RLU: Relative Lights Units

TMD: Transmembrane Domain

UV: Ultraviolet

YFP: Yellow Fluorescent Protein

1 Introduction

1.1 Melanoma

1.1.1 Generality

Melanocytes are mostly found in the basal layer of the epidermis. They are also present in hair follicles, uveal tract of the eyes, meninges and anogenital tract [1]. They produce the melanin, accountable for skin color, and which is transported to keratinocytes [1]. Different mechanisms for melanin transfer from melanocytes to keratinocytes have been described, however they all remain hypotheses. Melanocyte proliferation and pigment production are mediated by ultraviolet (UV) radiation as keratinocytes secrete α-melanocyte stimulating hormone after activation of p53 following DNA damages [1]. Melanin spreads and absorbs UV radiation allowing keratinocytes located in the epidermis to protect their nucleus from UV radiation-induced DNA damage [1].

Melanoma corresponds to an abnormal development of the melanocytes. Malignant melanocytes can lead to diverse types of melanoma classified depending on different criteria (e.g. cell of origin, pathogenesis, clinical aspect, histologic aspects, genetic alteration, etc.) [2]. It is possible to differentiate two main classes: epithelium associated melanoma and non-epithelium associated (**Figure 1**) [2]. Abnormal development of melanocytes results in a gain of function mutations in oncogenes (i.e. *NRAS*, *HRAS*, *BRAF*, *KIT*, *GNAQ*, *ALK*, *ROS1*, *RET*, *NTRK1*) however, the transition from intermediate to malignant tumor is usually a loss of function of tumor suppressor genes (i.e. *CDNK2A*, *TP53*, *PTEN*, *BAP1*) [2]. *BRAF* mutation is the most frequent in melanoma [2].

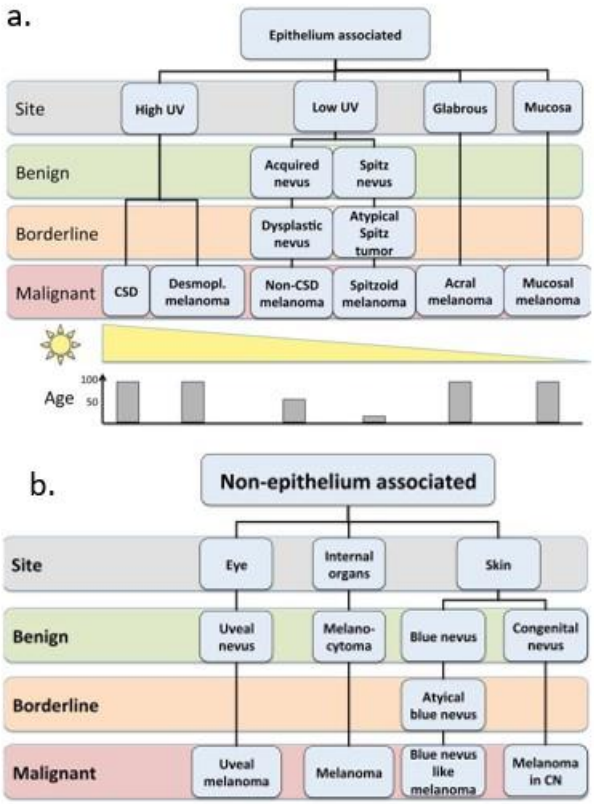

Figure 1 – Representation of the different type of abnormal development of melanocytes. a) Melanoma arising from epithelium-associated melanocytes. Three different stage are visible: benign, intermediate to malignant. Each class has different relationship to UV radiation and age distribution. b) Melanoma arising from non-epithelium associated melanocytes. Categories have no relationship to UV radiation and the age distribution is spread. Taken from Bastian, *et al.* [2].

It has been shown that exposure to intense sunlight might be responsible for the recent increasing of melanoma incidence worldwide [3]. Sun-exposed skin lead to the most common melanoma in Caucasians population [1]. This type of melanoma, chronic sun-induced damage melanomas (CSD melanomas), is usually located on the head, neck and dorsal surfaces of the distal extremities of people over 55 years old [1]. UV solar radiation has mutagenic effect on DNA promoting malignant change in the skin. It stimulates the cellular constituents of the skin to produce growth factors, reduces cutaneous immune defenses and promotes reactive oxygen species of melanin leading to DNA damage followed by a decrease of damaged cell's apoptosis [3].

1.1.2 Epidemiology

Melanoma has become an important public health issue in many countries. Since mid-1960s, melanoma incidence has risen by 3 to 8 percent per year [3]. It is usually diagnosed at the age of 50 but nowadays it is also diagnosed more frequently in younger adults and rarely in children [4]. It is the fastest growing cancer worldwide [5]. In Europe, cutaneous melanoma represents 1 to 2 percents of all malignant tumors [6]. The regions affected are predominantly those with Caucasian population and the highest incidences are in Australia and New Zealand followed by Northern America, Northern Europe and Western Europe [7]. In all these country, mortality has steadily increased (**Figure 2**) [8]. Besides geographic location, gender and genetic influence melanoma progression [8].

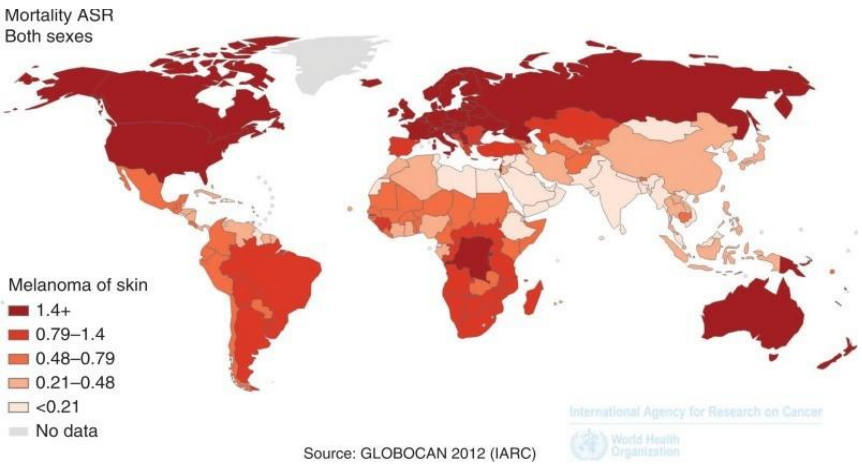

Figure 2 – Geographic representation of worldwide melanoma age standardized mortality rate (ASR). ASR is expressed per 100 000 persons. Taken from Matthews, *et al.* [8].

1.1.3 Treatment

There are different ways to cure melanoma (i.e. Surgical excision, radiotherapy, immunotherapy, interferon-based approaches, cytokines, adoptive immunotherapy, vaccines, immune checkpoint inhibitors, chemotherapy, targeted therapies) depending on the stage of the cancer at diagnosis [9]. For the early-stage melanoma, surgical excision is usually used [9]. However, metastatic relapse follows 20% of melanoma surgical resection leading to a poor prognostic [10]. As melanocytes are known to rapidly repair DNA damages induced by low-dose radiation, radiotherapy has been considered less efficient and its use remains controversial [9]. However, radiation is commonly applied in mucosal melanoma and in large aggressive lesions, more radiosensitives [9]. In other cases, radiotherapy is preferred for its palliative role as it lower pain, spinal cord compression from bone metastases or bleeding [10]. Immunotherapy, interferon-based approach, vaccines and cytokines are under investigation. Even if their future seems promising, for the time being, benefits doesn't overcome drawbacks and more clinical trials are needed [9] [10]. Immune check point inhibitor aims to interact with regulators of the immune system. Even though the response rate is promising, immune side effects have been described in many clinical trials [9]. Despite these cures, melanoma is an aggressive cancer and rapidly metastasize making a lot of treatments no longer sufficient [8]. Once cancer metastasizes, survival with treatment goes from 8 to 12 months [8].

Chemotherapy is the most common treatment. Nevertheless, melanoma cells often resist to conventional drug-based therapies [11]. Dacarbazine, temozolomide, paclitaxel, doxorubicin, tamoxifen, platinum analogs (i.e. Cisplatin, carboplatin) and nitrosoureas (i.e. Carmustine, lomustine, fotemustine) have demonstrated curative effects but chemoresistance in melanoma is an important obstacle and the response rate was found to be below 10% [2] [12]. Dacarbazine, a pro-drug metabolized in the liver, has been the first-line option for metastatic melanoma for years but outcomes remain lower than expected [10]. Combined chemotherapy showed an increase response rate up to 10% but overall survival remains poor [12]. A lot of alternative therapies have been investigated as the adoptive cell therapy (ACT) or targeted therapies. ACT recently showed above 40% response rate [13]. It is an infusion of anti-tumor lymphocytes collected in the patient and grown ex vivo to boost the immune response [13]. Targeted therapies have for goal to inhibit biochemical pathways activated by mutations in tumors cells. *BRAF* and *KIT* mutation has been highly studied and promising results have been shown [9]. Targeted therapies seem more successful as they either inhibit or activate a single target making it an easy approach [9]. However, melanoma complexity and numerous interactions make it more complex [9]. Better understanding of genetic variations in melanoma cells is needed.

1.2 Chemoresistance

1.2.1 Generality

Drug resistance is a wide challenge while treating cancer patients. It constitutes the first cause of failure for chemotherapeutic treatments of most human tumors [14]. It causes disease relapse and metastasis [15]. There are different mechanisms leading to chemoresistance (e.g. oncogenes, tumor suppressors, mitochondrial alteration, DNA repair, autophagy, epithelial-mesenchymal transition (EMT), cancer stemness, exosome, transporter pumps, local physiology variation) (**Figure 3**) [15] [16]. There are many cross talks between these aspects. Proteins encoded from oncogenes can modulate the expression of apoptosis-related genes leading to EMT, cell stemness and autophagy [15].

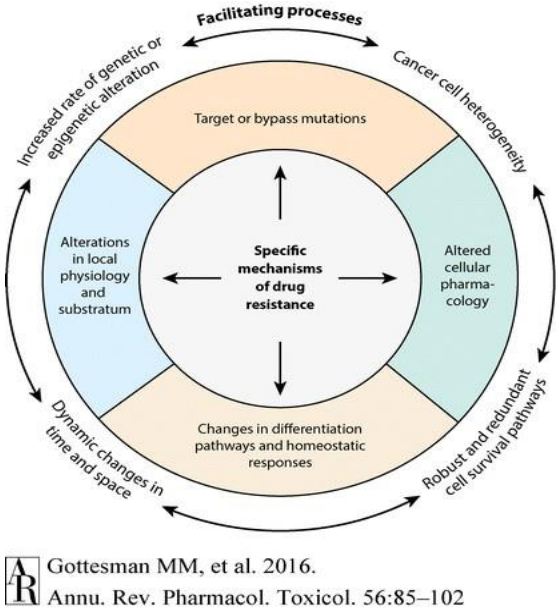

Figure 3 – Drug resistance process. It results from different mechanisms that make cells resistant to anticancer agents. All processes interact together in order to develop drug resistance in cancer cells. Taken from Gottesman, *et al.* [16].

1.2.2 Transporters

A well-known chemoresistance mechanism is mediated by membrane proteins that move out cytotoxic molecules leading to an intracellular concentration widely below an effective cell-killing amount [17]. Decrease of drug influx into the cells, increase of drug efflux from the cells and metabolism dysfunction can lead to a reduction of intracellular drug accumulation [14].

Some cancers develop resistance to drugs that are structurally and mechanistically unrelated. This is called multidrug resistance (MDR) [17]. The primary cause of MDR phenotype is due to the overexpression by tumor cells of some members of the ATP binding cassette transporter superfamily (**Figure 4**) [14]. These transporters, through increased efflux of chemotherapeutic agents, lead to the reduction of intracellular drug concentration and important drug insensitivity often to multiple agents [18]. The objective to lower MDR in cancer by pharmacological inhibition of certain ABC transporters has been quest for a long time [18]. However, results of clinical trials using modulators of multidrug transporters have given unsatisfactory outcome [18]. Verapamil and cyclosporine A were first used to inhibit ABC transporters, but they showed an unacceptable level of toxicity [18]. The fourth generation of inhibitors, Valspodar and Zosuquidar also led to disappointing results in clinical studies [18]. Some strategies, other than direct inhibition of the transporter, have a promising future to overcome MDR. Tyrosine kinase inhibitors interacting with ABC transporters, antibodies or nanoparticles showed potential benefits for cancer patients [17].

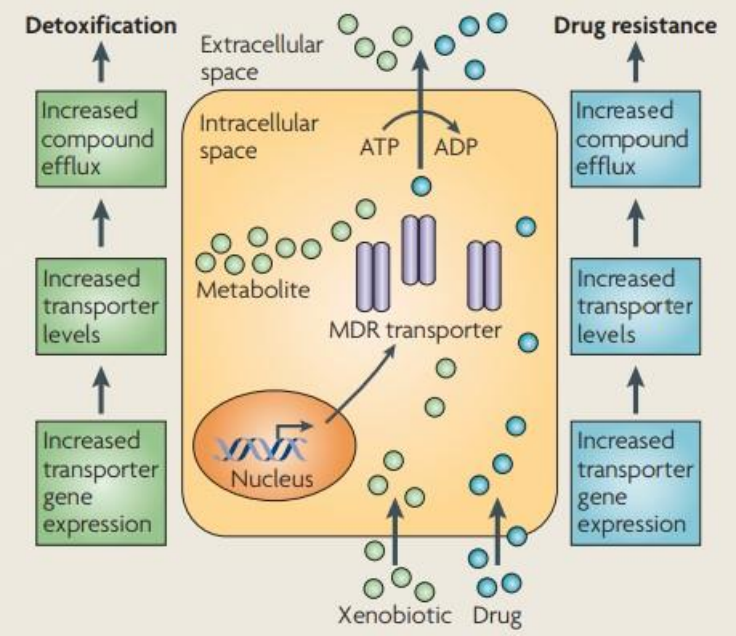

Figure 4 – ABC transporters role. One of the functions of ABC transporter is cells protection from toxic compounds entering the cell. However, this mechanism also allows cells to efflux out drugs leading to resistance to different chemotherapeutic agents in various cancer. Taken from Fletcher, *et al.* [18].

1.2.3 Chemoresistance in melanoma

As mentioned above, melanoma are highly resistant to conventional chemotherapy. In fact, treatment failure in melanoma is frequent and the involvement of ABC transporters might be the common cause [11]. ABC transporters, potentially linked with resistance, are expressed to a large degree in melanoma (e.g. ABCA5, ABCA9, ABCB1, ABCB5, ABCB6, ABCB8, ABCC1, ABCC2, ABCD1, ABCD2, ABCD3, etc.) [11] [19]. These transporters efflux out many chemotherapeutics from the cells [19]. However, the role of several transporters in melanocytes and melanoma remains unclear [19]. Their implication still needs to be elucidated and further studies are needed to highlight their role in order to decrease melanoma chemoresistance.

On the other hand, melanoma cells show an important difference. They have a lysosome-related organelle used for melanin synthesis called melanosome [11]. This organelle sequestrates toxic compounds produced in the course of melanin biosynthesis and is also implicated in drug export and sequestration [11]. It has been shown that melanosome sequestration of cytotoxic drug has an important impact on chemoresistance [20].

To a lower extend, other mechanisms are related to therapeutic resistance in melanoma. For example, increased DNA repair, oncogenes expression and gene increased methylation [11].

To overcome chemoresistance in melanoma, many therapies relying on mutations, signaling pathways and immunological response has been proposed [11]. However, drug resistance remains an important challenge.

1.3 ABC transporters

1.3.1 Generality

ATP Binding Cassette (ABC) transporters are primary active transporters. They transport a wide range of substrates (e.g. ions, peptides, amino acids, sugar, xenobiotics, etc.) and use the energy from ATP hydrolysis to translocate molecules across membranes against their chemical gradient [21]. ABC transporters are present in prokaryotes, fungi, plants yeast and animals [21]. They transport substrates out (efflux) of cells or in (influx) cells and organelles [21]. Eukaryotes's ABC transporters are only capable of export, while prokaryote ones play a role of importers and exporters [22]. ABC transporters either play a role in transport across the cell membrane or in intracellular compartmental transport [22]. In human, ABC transporters are encoded by 48 genes divided in seven families named from A to G and are expressed ubiquitously in the liver, intestine, blood-brain barrier, blood-testis barrier, placenta, kidney, etc... [21].

1.3.2 Structure of ABC transporters

The typical architecture of ABC transporters consists of two nucleotide-binding domains (NBD) and two transmembrane domains (TMD), each composed of 6 α-helices (**Figure 5**) [22]. NBDs are divided in a catalytic core domain that contains the conserved P-loop (also called Walker A motif), the Walker B motif, the Q-loop, the H-motif and an α-helical domain that contains the LSGGQ motif (C motif), which is the characteristic signature for the NBDs of ABC transporters (**Figure 5**) [22]. The Walker A and B motifs participate in the binding of the nucleotide phosphates and the $Mg2^{+}$ necessary for the hydrolysis of ATP [22]. Such a four domain structure (two NBD and two TMD) is defined as a full ABC transporter. In a full transporter, the ABC subunits pack together in a "head-to-tail" way such that the Walker A of one subunit is oriented towards the signature motif of the other [22]. There are some exceptions to this typical conformation. Some member of the ABCC family possess an additional TMD with 5 α-helices at the N-terminal side of the protein (e.g. ABCC1, C2 and C6) (**Figure 6**) [23].

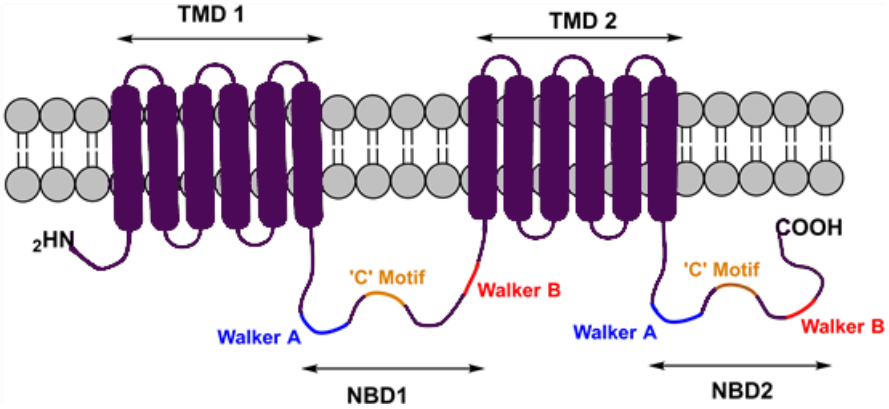

Figure 5 – Typical full ABC transporter. ABCC5 topology showing both trans membrane domains (TMD), both nucleotide binding domains (NBD), the Walker A in blue, C loop in orange and Walker B in red. Taken from Singh, *et al.* [24].

Beside full ABC transporters, half transporters also exist and contain one NBD and one TMD (**Figure 6**). The NBD is either at the N- or C- terminal site of the TMD (i.e. ABCG family and ABCB2, B3, B6 to B10, D1 to D4 respectively) [21]. They must homo- or heterodimerize to be functional [25]. In fact, individual subunits are unable to correctly bind and hydrolyze ATP [22].

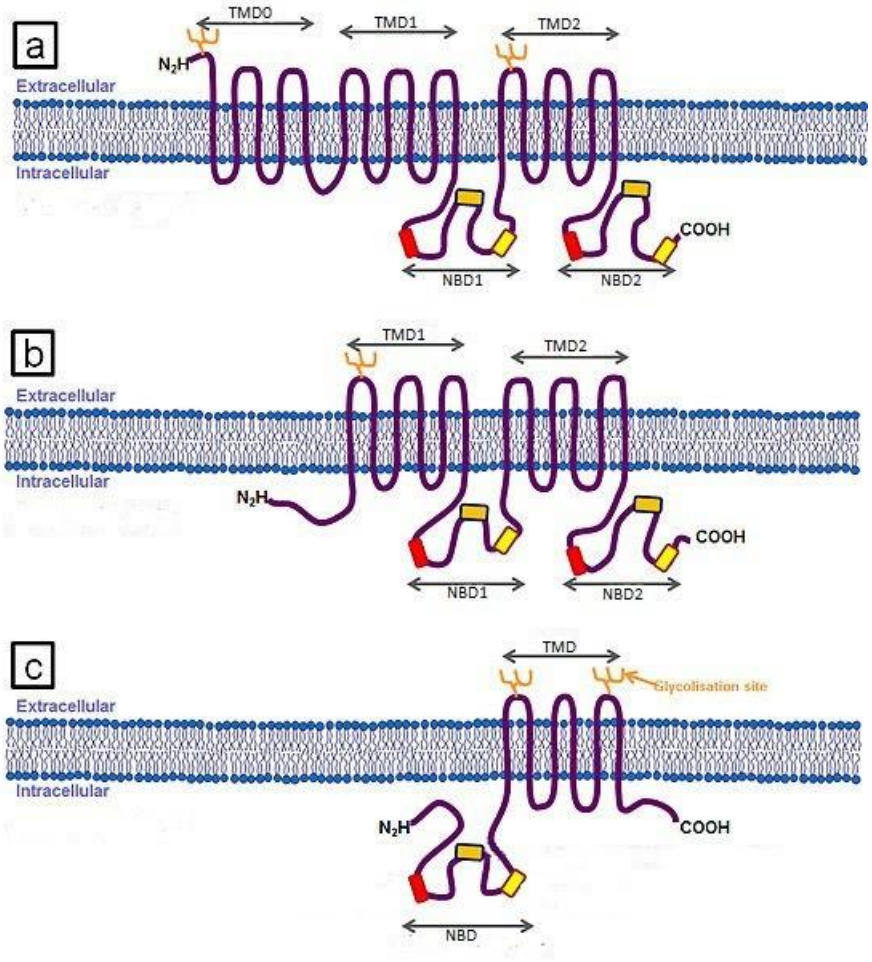

Figure 6 – Different conformations of ABC transporters. The TMD is composed of six α-helices. The NBD is composed of conserved motifs as Walker A, C motif and Walker B. a: Long ABC transporters have three TMD and two NBD (e.g. ABCC1). b: Typical ABC full transporters are composed of 2 TMD and 2 NBD (e.g. ABCB1). c: Half ABC transporter have 1 TMD and 1 NBD (e.g. ABCG2). Taken from Erdelyi-Belle, *et al.* [26].

Finally, there are soluble ABC proteins, which lack TMDs (e.g. ABCE1, ABCF family) [21]. The lack of TMD makes it unlikely that these proteins functions as transporters. For the time being, no diseases have been associated with either of these soluble ABC proteins [21].

1.3.3 Catalytic cycle

The catalytic cycle of these transporters consists of the substrate liaison to the binding pocket of the TMD, and the ATP binding in the two NBDs [22]. Substrate specificity for each transporter is determined by the amino acid sequence in the TMD [27]. These bindings are followed by the hydrolysis of one ATP molecule, which leads to a conformational change, and the substrate release from the protein [22]. The second molecule of ATP is then hydrolyzed, which results in a conformational reset of the protein [22]. Basal ATP hydrolysis drives a continuously changing conformation that facilitate substrate binding and transport. The TMD of the ABC transporters are highly versatile, allowing them to recognize many different substrates [21].

1.3.4 Diseases implication

ABC transporters are well-known to be concerned by the movement of most drugs and metabolites across membranes making them important in terms of cancer therapy, pharmacokinetics and pharmacogenetics [21]. However, in addition to that, mutations in the ABC genes are involved in several severe diseases (**Table 1**) [28] [27].

Disease	Transporter
Cancer	ABCB1, ABCC1, ABCG2
Cystic fibrosis	ABCC7
Stargardt disease and age-related macular degeneration	ABCA4
Tangier disease and familial HDL deficiency	ABCA1
Progressive familial intrahepatic cholestatis	ABCB4, ABCB11
Dubin-Johnson syndrome	ABCC2
Pseudoxanthoma elasticum	ABCC6
Persistent hypoglycemia of infancy	ABCC8, ABCC9
Sideroblastic anemia and ataxia	ABCB7
Sitosterolemia	ABCG5, ABCG8
Adrenoleukodystrophy	ABCD1
Immune deficiency	ABCB2, ABCB3
Dyschromatosis universalis hereditaria	ABCB5, ABCB6

Table 1 – Human diseases associated with ABC transporters [28].

ABC transporters have been extensively studied for their role in cancer multidrug resistance were the cancer cell has not only become resistant to the administered drug(s), but also to a wide panel of drugs which are structurally and mechanistically unrelated (MDR). However, a growing body of evidence indicated that ABC transporters are also involved in the underlying mechanisms of tumorigenesis [18]. For instance, correlation of ABCC1 overexpression with tumor size was highlighted in breast cancer and increase ABCB1 levels correlate with invasion into vessels of colorectal carcinomas cancer cells [18]. It was reported that an $ABCB5^{+}$ melanoma cell subpopulation shows a different tumorigenic capacity compared with $ABCB5^{-}$ melanoma cells [29]. Different explanations have been proposed regarding the implication of ABC transporters in tumorigenesis (e.g. release of signaling molecules and hormones, redox status regulation, release of nutrients and metabolism regulation, membrane lipid composition regulation, paracrine regulation of the tumor microenvironment) [30]. Overall, it became clear that ABC transporters have an impact in cancer cell proliferation, differentiation, invasion, migration and malignant potential [30].

Indeed, cancer cells show different capabilities: self-sufficiency in growth signals, insensitivity to anti-growth signals, evasion of apoptosis, limitless replicative potential, sustained angiogenesis, tissue invasion and metastasis, cancer related inflammation [18]. Some observations lead to the conclusion that ABC transporters might play a role in some of these cancer characteristics [18]. Moreover, lipids with established roles in tumor biology (e.g. prostaglandins, leukotrienes, sphingosine-1-phosphate) are known or suspected to be ABC substrates, leading to whether ABC transporters mediated efflux of these molecules influences cancer outcome [18].

1.4 ABCB Family

This family of 11 genes is composed of three full transporters (e.g. ABCB1, ABCB4, ABCB11), seven half transporters that must either homo- or heterodimerize to be functional (e.g. ABCB2, ABCB3, ABCB6, ABCB7, ABCB8, ABCB9, ABCB10) and ABCB5, that can be found as a full or a half transporter [31]. It is the only ABC family containing both full and half transporters [27]. This family is unique to mammals and is also known as multidrug resistance (MDR) family because numerous members of the ABCB family confer multidrug resistance in cancer cells [21].

ABCB1, also called MDR1, was the first ABC transporter characterized [27]. It is localized in the blood-brain barrier and the liver and it is largely implicated in multidrug resistance [27].

ABCB2 and ABCB3, respectively TAP1 and TAP2, are half ABC transporters. They heterodimerize in order to move peptides into the endoplasmic reticulum [27]. After proteasomal degradation, peptides are generated in the cytosol and translocated in the endoplasmic reticulum by TAP1 and TAP2 for presentation to the Major Histocompatibility Complex (MHC) class I molecules [32].

ABCB4, known as MDR2, is located in the liver [27]. This transporter transports phosphatidylcholine into bile [33].

ABCB6, first localized in the outer membrane of mitochondria, has been shown to be expressed in the membrane of lysosomes and melanosomes [34]. A mutation in ABCB6 is linked with different diseases such as ocular coloboma and porphyria [34]. The prevention of ABCB6 expression brings about decrease of cellular melanin contents leading to the conclusion that it might be implicated in melanogenesis [34].

ABCB7, localized in the mitochondria, is involved in the transport of iron and sulfur [35]. Iron and sulfur play a significant structural and catalytic role in mitochondria. A mutation in ABCB7 leads to sideroblastic anemia [35]. ABCB7 knock out mice resulted in non-viable embryos with development issues and hemorrhage [35].

ABCB8 is located in the mitochondrial inner membrane and is involved in peptides transport and intracellular trafficking [32]. It's a component of the mitochondrial K_{ATP} channel and has a potential role in antigen processing and oxidative stress protection in cardiac cells [32] [36]. Moreover, ABCB8 plays an important role in multidrug resistance by the efflux of doxorubicin in different cancers [36].

ABCB9, also called TAP-Like, is located on lysosomes [27]. This transporter has structural similarities with TAP1 and TAP 2 [32]. However, it seems that it is not involved with the MHC class I and there is little information about its physiological role [32]. ABCB9 is largely expressed in Sertoli cells in the testis [37]. Sertoli cells show significant secretory and phagocytosis activities potentially associated with ABCB9 [37].

ABCB10, as ABCB8, is located in the mitochondrial inner membrane and involved in peptides transport [32]. ABCB10 seems to homodimerize to become efficient [32]. ABCB10 could prevent mitochondrial dysfunction induced by accumulation of peptides [36]. It also plays a role in heme and iron metabolism, while giving specific antioxidant function [36].

ABCB11, also named BSEP, is like ABCB4, involved in bile acids secretion and located in the liver [27].

1.5 ABCB5

ABCB5 is a member of the ABCB family expressed in melanocytes, retinal pigment epithelial cells, testis and uterus [11]. It has also been found in different cancers (i.e. melanoma, breast cancer, colorectal cancer, leukemia and hepatocellular carcinoma) [38]. ABCB5 transports different substrates including chemotherapeutics (as doxorubicin) leading to multidrug resistance [39]. ABCB5 is a marker of cancer stem cells and it might be involved in melanoma progression [39]. Studies performed in melanoma cell lines, either mutation of ABCB5 or loss of ABCB5 expression, showed an increased proliferative and invasive capacities of tumor cells suggesting that ABCB5 is a potential tumor suppressor gene [40]. Eleven ABCB5's transcripts have been identified, among which three major groups have been described [31]. It's the only known ABC transporter to be present in three different conformations: as a full, a half-like transporter and as a soluble protein [31].

The ABCB5FL (1257 aa) encodes a full transporter mainly expressed in the prostate and testis [31]. The ABCB5β (812 aa) encodes a half-like transporter, composed of one TMD flanked by two NBDs, which is the unique feature of this transporter (**Figure 7**) [38]. Furthermore, the N-terminal NBD lacks a conserved Walker A motif, which precludes the binding of ATP and its hydrolysis [38]. ABCB5α (131 aa) and other small fragments encode soluble proteins, for which the cellular role has yet to be unraveled [41].

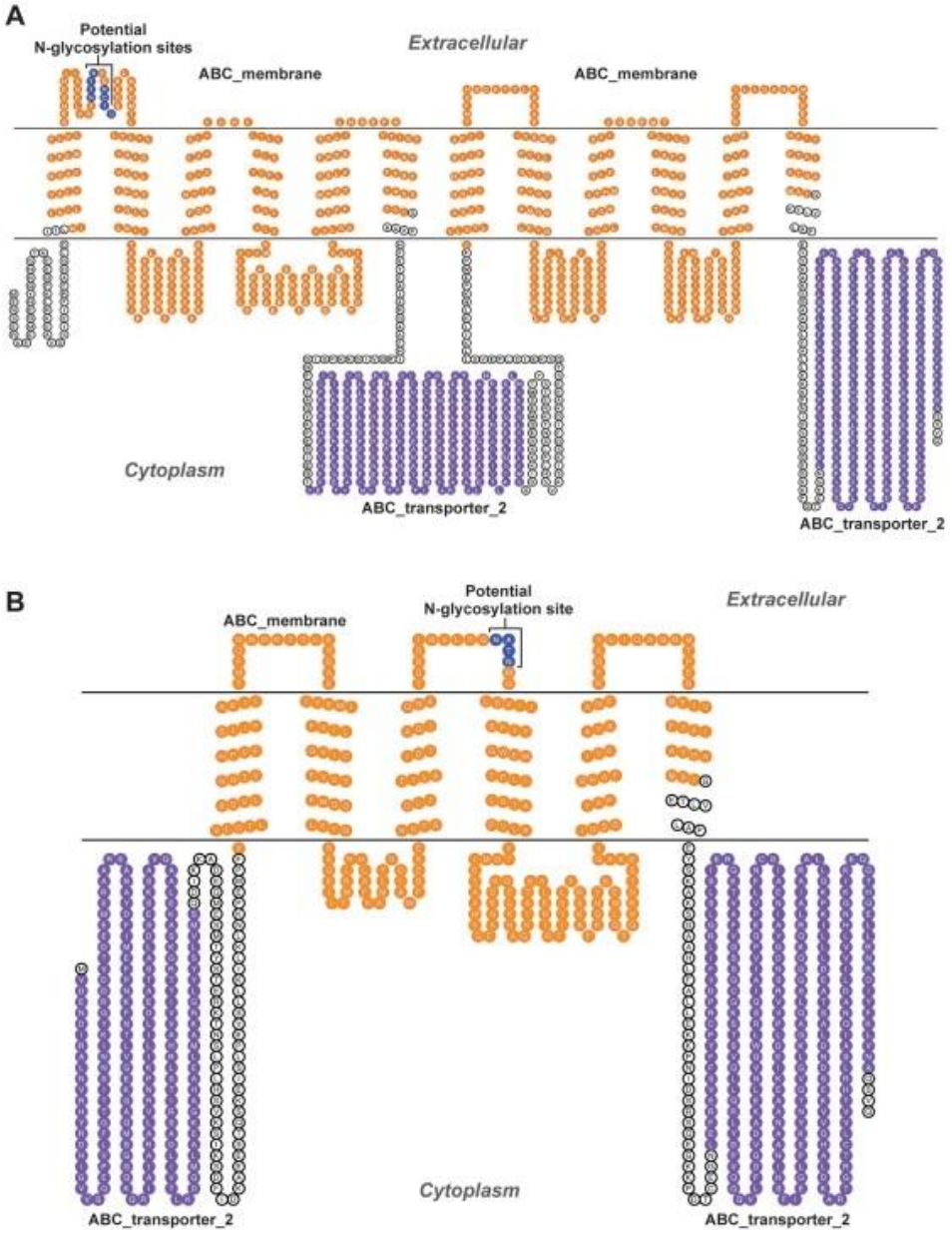

Figure 7 – Predicted structures of ABCB5. a: ABCB5 FL composed of 12 TMD and 2 NBD. Two N-glycosylation sites are highlighted in blue. b: ABCB5*β* composed of 6 TMD and 2 NBD. One N-glycosylation site is highlighted in blue. Taken from Moitra, *et al.* [38].

Moreover, ABCB5*α* and ABCB5*β* are not expressed in amelanotic melanomas, suggesting that these two transcripts are involved in melanin synthesis [11]. It has been highlighted that ABCB5, among other ABC transporters, isolate cytotoxic melanin intermediates into subcellular compartment (e.g. Endosomes, lysosomes, melanosomes) (**Figure 8**) [11]. ABCB5, in melanoma, correlates with drug efflux of several compounds leading to drug resistance [42].

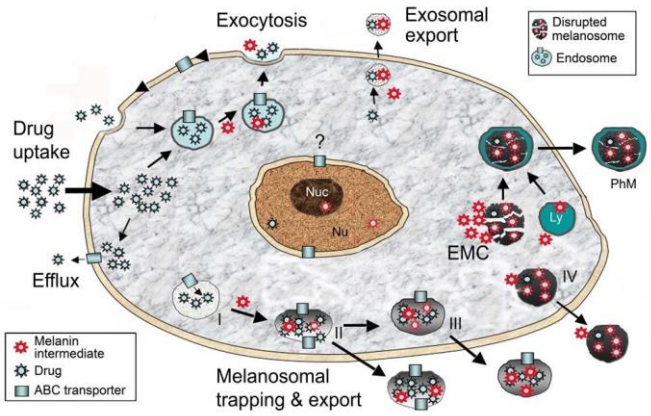

Figure 8 – Melanocytes homeostasis mediated by ABCB5 and other ABC transporters. They obstruct cytotoxic melanin intermediates into subcellular compartment (endosomes, lysosomes and melanosomes). These organelles are then exported from cells. The same mechanism is used by melanoma cells to confer drug resistance as they used ABC transporters to trap cytotoxic compounds in organelles. Taken from Chen, *et al.* [11].

ABCB5*β* might form a dimer to create a functional transporter. Potential dimerization motifs were identified in its N-terminal region [38]. In contrast with ABCB5FL, which mediates resistance to taxanes and anthracyclines, the ABCB5*β* homodimer cannot confer drug resistance, and does not appear to be a functional transporter [43]. In our laboratory, Lefèvre and colleagues investigated the potential heterodimerization of ABCB5*β* with ABCB6 and ABCB9 [44]. Different common points between these half transporters exist. ABCB6 colocalizes with ABCB5*β* in melanocytes and is involved in melanin synthesis. ABCB6 or ABCB5*β* mutations have been found to be associated with *dyschromatosis universalis hereditaria*, an inherited genetic skin condition [34] [45]. ABCB9 colocalizes with ABCB5*β* in Sertoli cells and is a lysosome-related transporter [37]. The ABCB6 and ABCB9 constructs were co-transfected in HEK293T cells along with the mCherry-tagged ABCB5*β* construct. Coimmunoprecipitation experiments revealed that ABCB5*β* heterodimerizes with both ABCB6 and ABCB9, see **Figures 9 - 12**, adapted from Figures 14 and 15 in Lefèvre, *et al* [44]. These results need to be validated with another protein-protein interaction assay.

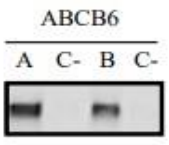

Figure 9 – Co-immunoprecipitation performed by precipitation of ABCB6 followed by the revelation of ABCB5*β* using an anti-mCherry antibody, from the co-transfected cell lysates (A) and ABCB5*β* transfected cell lysates (B), showing heterodimerization of these half transporters revealed by a band at 120 kDa, which is not present in the IgG controls (C-). Taken from Lefèvre, *et al.* [44].

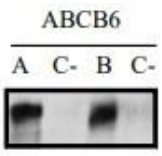

Figure 10 – Co-immunoprecipitation performed by precipitation of ABCB6 followed by the revelation of ABCB5*β* using an anti-ABCB5*β* antibody, from the co-transfected cell lysates (A) and ABCB5*β*-transfected cell lysates (B), showing heterodimerization of these half transporters revealed by a band at 120 kDa, which is not present in the IgG controls (C-) Taken from Lefèvre, *et al.* [44].

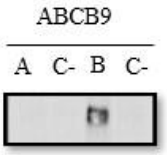

Figure 11 – Co-immunoprecipitation performed by precipitation of ABCB9 followed by the revelation of ABCB5β using an anti-mCherry antibody, from the co-transfected cell lysates (A) and ABCB5β-transfected cell lysates (B), showing heterodimerization of these half transporters revealed by a band at 120 kDa, which is not present in the IgG controls (C-) Taken from Lefèvre, *et al.* [44].

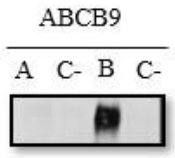

Figure 12 – Co-immunoprecipitation performed by precipitation of ABCB9 followed by the revelation of ABCB5β using an anti-ABCB5β antibody, from the co-transfected cell lysates (A) and ABCB5β-transfected cell lysates (B), showing heterodimerization of these half transporters revealed by a band at 120 kDa, which is not present in the IgG controls (C-) Taken from Lefèvre, *et al.* [44].

1.6 Protein-Protein interaction investigation

1.6.1 Forster Resonance Energy Transfer (FRET)

Forster resonance energy transfer (FRET) is an energy transfer between a donor and an acceptor in close proximity named after the German scientist Theodor Forster [46]. The energy goes from one molecule to another by non-radiative transfer [46]. It can be called fluorescence resonance energy transfer when both donor and acceptor are fluorescent. The transfer is possible depending on different parameters (**Figure 13**). First, the donor and the acceptor need to be separated by less than 10 nm [47]. Second, there must be an overlap of the donor emission and acceptor absorption spectra [47]. Finally, the orientation of the acceptor and the donor have an influence on the intensity [47].

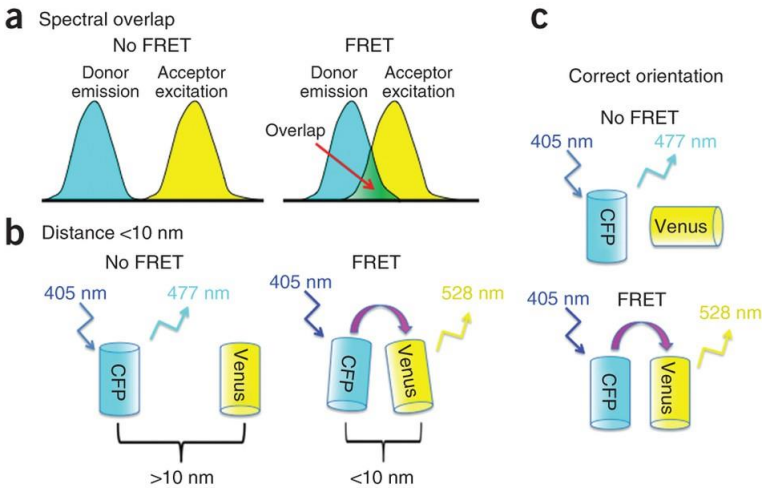

Figure 13 – Parameters influencing FRET efficiency. Cyan fluorescent protein (CFP) is donor and Venus is acceptor. a: Spectral overlap of the donor and the acceptor spectra is needed. b: Separation of the donor and the acceptor smaller than 10 nm is essential. c: Correct orientation of the acceptor towards the donor must be respected. Taken from Northwestern University [48].

The most frequent combination of fluorophores used are the green fluorescent protein (GFP) and the yellow fluorescent protein (YFP) [49]. However, FRET present some drawbacks. The major one is that it requires extrinsic excitation with a suitable light source, which can lead to photobleaching, autofluorescence or simultaneous excitation of both donor and acceptor fluorophores [50]. Moreover, because FRET signals are usually weak, several controls and careful interpretation of their measurement are needed [46].

FRET has already permitted to identify heterodimerization between the ABC transporters ABCD1 and ABCD3 (respectively called ALDP and PMP70) [25]. Cyan fluorescent protein (CFP) and yellow fluorescent protein (YFP) were used as donor and acceptor. This result paves the way to energy transfer method as a method to assess ABC transporter dimerization behavior.

1.6.2 Bioluminescence Resonance Energy Transfer (BRET)

Bioluminescence resonance energy transfer (BRET) is a natural process that can be observed in marine species such as in the jellyfish *Aequorea victoria* [51]. It consists in the transfer of energy from a donor enzyme to a suitable acceptor molecule after substrate oxidation [50]. The bioluminescent protein oxidizes the substrate, which reaches its excited state and by after releases an electron. This electron goes to the fluorescent molecule which emits light at a particular wavelength (**Figure 14**). In order to be effective, the donor enzyme and acceptor molecule must be in close vicinity, less than 10 nm distance, as for the FRET (**Figure 14**) [50]. In BRET, false-negative signals associated with misfolding of the reconstituted protein and false-positive signals arising from nonspecific association of the split fragments are significantly reduced [52]. BRET avoid previously discussed drawbacks of FRET as there is no need of extrinsic excitation.

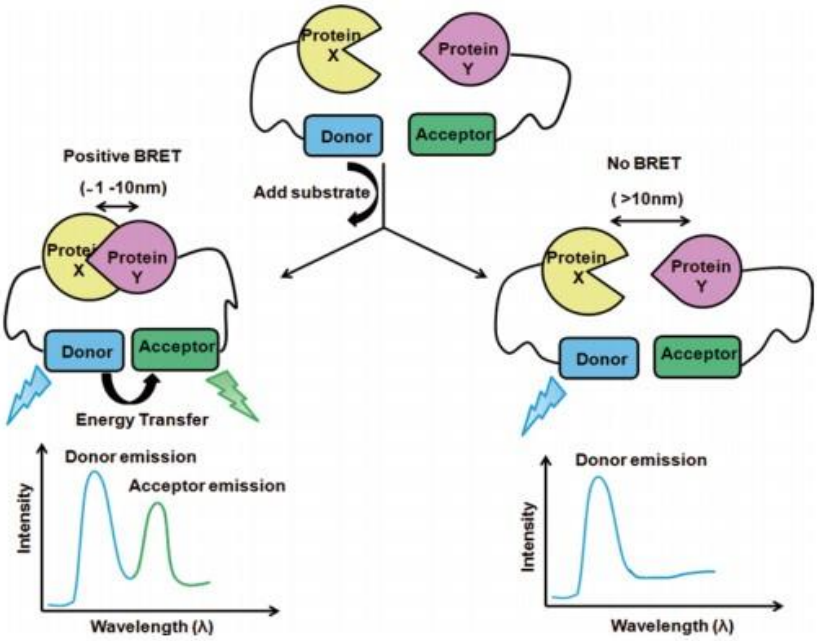

Figure 14 – Representation of the BRET assay. Protein X and Y are tagged with donor and acceptor. When the substrate is added both proteins need to be closer than 10 nm to see a transfer of energy. The transferred energy excites the acceptor who then emits light at a special wavelength. Intensity of the donor and acceptor emission can be measured. Taken from Dimri, *et al.* [53].

BRET assay was introduced for biological research in the late 1990s [53]. Its sensitive and rapid measurements make it a popular genetic reporter-based assay for protein-protein interaction studies [53]. The most common combination of donor-acceptor used are the *Renilla* luciferase as donor and GFP as acceptor [53]. However, both fluorophores give a weak signal leading to the implementation of NanoBRET assay.

1.6.3 Nano Bioluminescence Resonance Energy Transfer (NanoBRET)

Nano Bioluminescence resonance energy transfer (NanoBRET) stems from the BRET abovementioned but has been further optimized, allowing a better spectral separation between both fluorophores and an enhanced signal improving the results [54]. Sensitivity and dynamic range are increased as well as performance [55].

NanoBRET uses NanoLuc as a donor and HaloTag as an acceptor (**Figure 15**). NanoLuc is a luciferase engineered from the luciferase found in deep sea shrimp [56]. NanoLuc weight 19 kDa and is capable of producing very bright and sustained luminescence [57]. It also has a high physical stability. It is as efficiently expressed inside or outside of cells because its stability does not rely on disulfide bond [57]. Moreover, its small size makes it well suited for protein fusion tag [57]. On the other hand, HaloTag is a haloalkane dehalogenase [58]. HaloTag weight 33 kDa and is known to link covalently, in an irreversible way and in a very short time, to different ligand [58]. NanoLuc is, in consequence, a first choice experiment for studying protein-protein interactions.

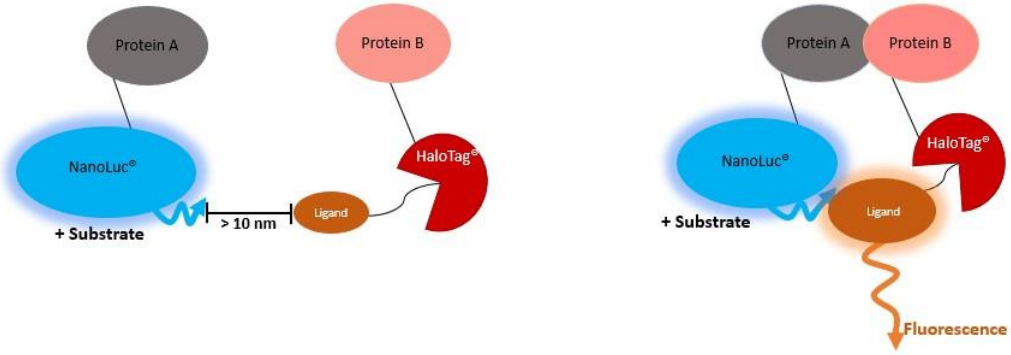

Figure 15 – Description of energy transfer from a NanoLuc® protein A fusion (energy donor) to a fluorescently labeled HaloTag® protein B fusion (energy acceptor). Ligand, HaloTag® NanoBRET™ 618 ligand, is covalently bond to the HaloTag® protein. If both proteins aren't closer than 10 nm, none NanoBRET will happen. Figure inspired by Promega NanoBRET PPI starter system [54].

2 Objectives

This work aims to validate both ABCB5*β*/ABCB6 and ABCB5*β*/ABCB9 heterodimers using the NanoBRET method. Indeed, each transporter share similarities with ABCB5*β* as previously mentioned and ABCB5*β*/ABCB6 and ABCB5*β*/ABCB9 heterodimerization was already highlighted by co-immunoprecipitation (**Figure 9 - 12**) [44].

In order to assess potential interactions, the NanoLuc and HaloTag tags had to be fused to the target proteins (ABCB5*β*, ABCB6, ABCB9). The first step of the project consists thenceforth in cloning cDNA of interest into NanoLuc® and HaloTag® vectors. As NanoBRET results depend on NanoLuc® /HaloTag® orientation and accessibility, both cDNAs must be cloned in N- and C-terminal part of each tag sequence in order to minimize chances of false negative results. Each combination of plasmids (36 in total, eight for each heterodimer and four for each homodimer) has then to be tested by transfection into HEK293T cell line (**Annex 1**). Afterwards, cells are seeded in 96 well plate and NanoBRET HaloTag® 618 ligand is then added. Each combination is tested with the ligand and without (as negative control). The day after, NanoLuc® substrate is added to the cells, donor and acceptor signals are measured on a dual filter at 447 nm and 610 nm. Next, the NanoBRET corrected ratio is calculated, which is the difference between the ratio 610nm/447nm of the ligand-containing sample and the ratio 610/447 nm of the control sample [54].

$$NanoBRET\ Corrected\ Ratio = (Ligand\ \frac{610\ \text{nm}}{447\ \text{nm}}) - (No\ ligand\ control\ \frac{610\ \text{nm}}{447\ \text{nm}})$$

The best combination is then be selected and further optimized for relative levels of the acceptor and donor fluorophores. If it turns out that the two proteins show a NanoBRET ratio suggesting that they interact together, this combination will have to take a donor dilution assay and thereafter will have to be validated by a donor saturation assay.

Donor dilution assay decreases the free donor amount in HEK293T cells. Different dilution of the donor, NanoLuc® DNA, is used (i.e. 1:1 NanoLuc® to HaloTag®, 1:10, 1:100, 1:1000). This step allows us to determine the optimal NanoLuc and HaloTag DNA ratio showing the best dynamic range [54].

To establish assay specificity, a donor saturation assay is needed. Indeed, both proteins might be in close proximity without interacting together, resulting in a non-specific BRET ratio. This phenomenon is known as the Bystander effect, which corresponds to the biological response of a cell because of an event nearby [59]. Therefore, donor saturation assay had to be performed. Different amount of the acceptor, HaloTag® DNA, is used (**Table 2**). If signal increases linearly with growing amount of acceptor, while amount of donor remains constant, the BRET result will be considered as nonspecific (**Figure 16**) [54]. Contrariwise, if signal increases in a hyperbolic way and reaches a plateau, meaning that all donors are saturated with acceptor molecules, BRET signal will be considered as specific (**Figure 16**) [54].

NanoLuc DNA concentration (μg)	HaloTag DNA concentration (μg)	Ratio
0,20	1,777	133,3
0,20	0,790	39,5
0,20	0,351	26,4
0,20	0,156	7,8
0,20	0,069	3,4
0,20	0,030	1,5
0,20	0,013	0,65
0,20	0,006	0,3
0,20	0	0

Table 2 – NanoLuc and HaloTag DNA concentration used for the Donor saturation assay of each pair selected.

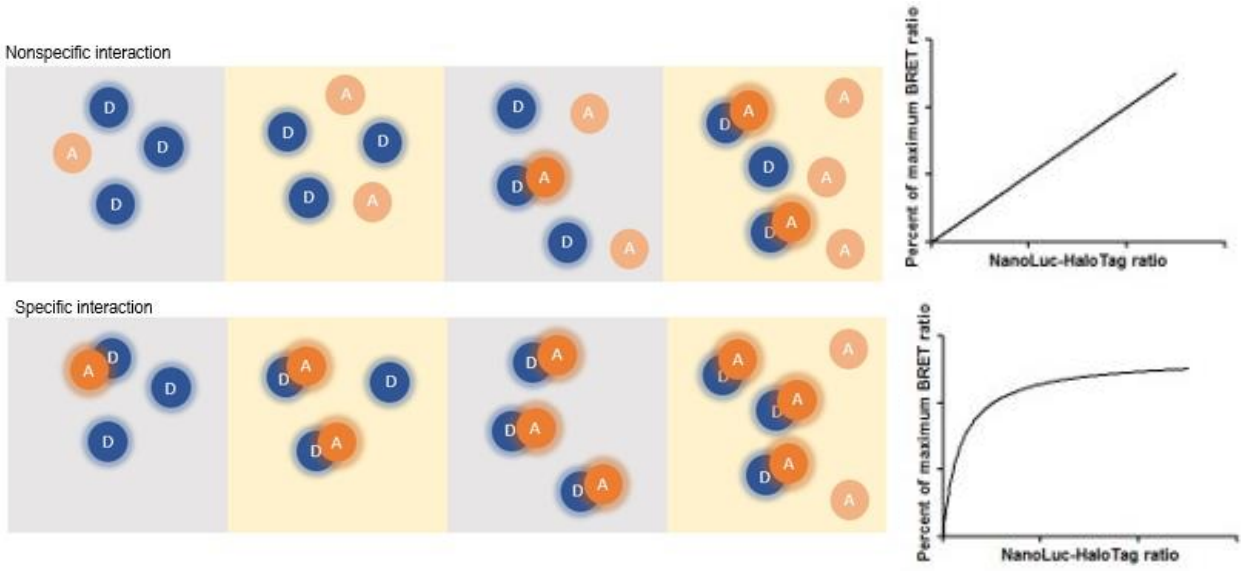

Figure 16 – Depiction of Donor saturation assay. The assay aims to determine the specificity of an interaction by adding growing amount of acceptor while keeping the amount of donor constant. Nonspecific interactions will exhibit linear evolution whereas specific interaction will follow hyperbolic evolution. Donor are in Blue (D) and acceptor are in orange (A). Figure inspired by Promega NanoBRET PPI starter system [54].

To summarize, ABCB5β, ABCB6 and ABCB9 cDNA sequences are cloned into plasmids containing NanoLuc ^{R} or HaloTag ^{R} in N- or C-terminal. All combinations of plasmids are then tested and cotransfected in HEK293T cells. The combination showing the best NanoBRET ratio is selected and further investigated. Indeed, if a combination exhibits a sufficient NanoBRET ratio, specificity of the interaction is assessed by a donor dilution assay and a donor saturation assay.

The confirmation of such an interaction between ABCB5β with ABCB6, and ABCB9 will shed some light on the biology of ABCB5β. How this half-like transporter becomes functional and where it localizes in the cell. Such data will contribute to better understanding of its role in normal and cancer cells.

3 Materials and Methods

3.1 DNA Construct

ABCB6, ABCB9 and ABCB5β cDNAs were inserted into the pCDNA3.1 expression vector and subcloned into the NanoLuc pNLF1-N[CMV/Hygro] and pNLF1-C[CMV/Hygro] Vectors, and the HaloTag pHTN HaloTag CMV-neo and pHTC HaloTag CMV-neo Vectors (**Figure 17 - 18**).

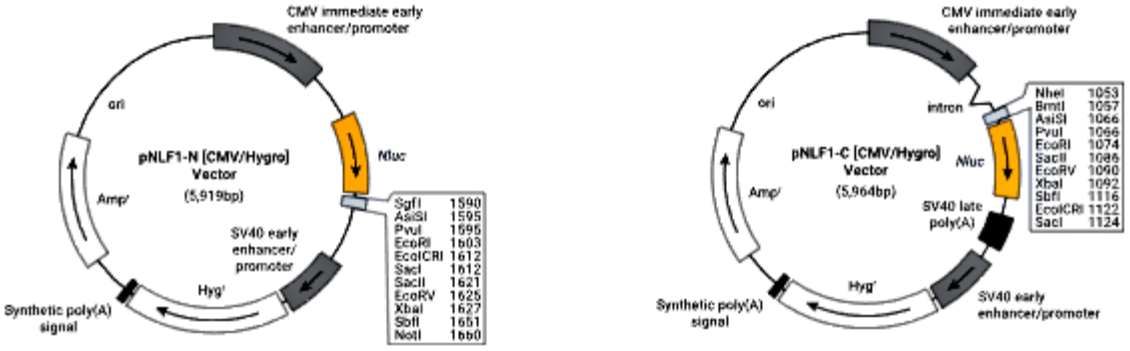

Figure 17 – Promega NanoBRET PPI starter systems's plasmids, NanoLuc plasmid. Left panel: pNLF1N[CMV/Hygro] Vector and right panel: pNLF1-C[CMV/Hygro] Vector. Taken from Promega NanoBRET PPI starter system [54].

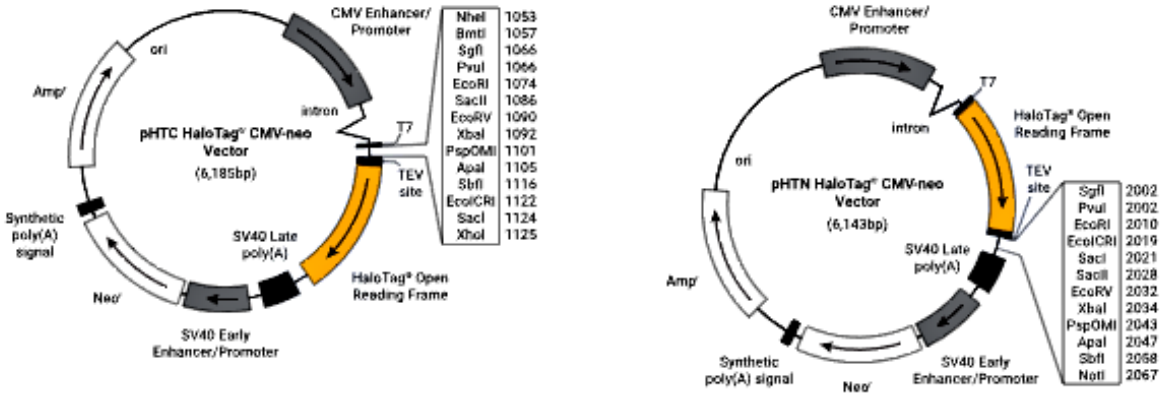

Figure 18 – Promega NanoBRET PPI starter systems's plasmids, HaloTag plasmid. Left panel: pHTC HaloTag CMV-neo Vector and right panel: pHTN HaloTag CMV-neo Vector. Taken from Promega NanoBRET PPI starter system [54].

In these constructs, ABCB6, ABCB9 and ABCB5*β* were inserted in the N- or C-terminal region of the tag (**Figure 19**). The constructs were fully verified by sequencing.

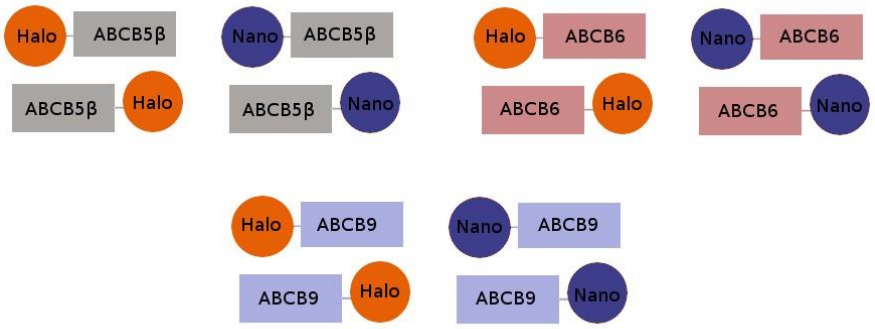

Figure 19 – Different combinations of HaloTag (Halo) and NanoLuc (Nano) plasmids with ABCB5*β*, ABCB6 and ABCB9 in C- and N- terminus.

3.1.1 Polymerase Chain Reaction

Primers used for the PCR were designed by serial cloner 2.1 (**Table 3**). They are 20 to 25 base pair long and have a melting temperature of approximatively 60˚C. Restriction enzymes cutting sites were also added. The restriction enzymes were chosen in the multiple cloning site of the plasmid. This step allows the PCR product to be further inserted into the plasmid. 12,5 *µL* of GoTaq DNA Polymerase (Promega, Madison, USA), 1,3 *µL* of each primer 10 *µ*M (reverse and forward), 9 *µL* of water and 1 *µL* of DNA template (ABCB5*β*, ABCB9 or ABCB6) were mixed together. The mix was placed in the PCR machine (C1000 Touch*TM* Thermal Cycler, BioRad, Hercules, USA). Finally, the amplification was programmed as presented in **Table 4**.

ABCB transporter and primer	Sequences (5’ - 3’)	Tm (˚C)
ABCB6 cter reverse	GGGGGAATTCCCGTTCCATGGTCTGAGG	60,4
ABCB6 cter forward	GGGGGCTAGCATGGTGACTGTGGGCAACTA	62,4
ABCB5 cter reverse	GGGGGAATTCTCACTGCACTGACTGTGCATTCA	63,8
ABCB5 cter forward	GGGGGCTAGCATGGTGGATGAGAATGACATCAGAGC	60,0
ABCB9 cter reverse	GGGGGAATTCGGCCTTGTGACTGCC	61,0
ABCB9 cter forward	GGGGGCTAGCATGCGGCTGTGGAAGG	64,0
ABCB6 nter reverse	CCCCGCGGCCGCTCACCGTTCCATGCTCTGA	59,8
ABCB6 nter forward	GGGGGAATTCATGGTGACTGTGGGCAACTA	60,9
ABCB5 nter reverse	GGGGGCGGCCGCTCACTGCACTGACTGTGCATTCA	61,7
ABCB5 nter forward	GGGGGAATTCATGGTGGATGAGAATGACATCAGAGC	61,8
ABCB9 nter reverse	CCAGGAGACAAGCTTCTTTGAG	58,0
ABCB9 nter forward	GGGGGAATTCATGCGGCTGTGGAAGG	61,0

Table 3 – Primers information.

Time	Temperature
3 minutes	95˚C
30 seconds 30 seconds 1 minute	95˚C 57˚C 72˚C 32 repetitions
10 minutes	72˚C

Table 4 – PCR program.

3.1.2 DNA Digestion

A digestion of the plasmids and inserts was performed. For the inserts, in each Eppendorf tube, 42 μL of the PCR product, 10 μL of the Buffer (Cut smart^{TM} buffer, New England Biolabs, Ipswich, USA), 1,5 μL of each enzyme and 45 μL of water were mixed together (**Table 5**). For the plasmids, in each Eppendorf tube, 16 μL of the plasmid, 10 μL of the Buffer, 1,5 μL of each enzyme and 71 μL of water were mixed together. All samples remained at 37˚C for one hour (**Table 5**).

Position	Enzyme	Enzyme
C terminus	Nhe1	EcoR1
N terminus	Not1	EcoR1

Table 5 – Restriction enzymes

3.1.3 DNA Dephosphorylation

While the digested insert remained at 37˚C, plasmids were dephosphorylated. This step was performed to avoid a number of non-recombinant plasmids. 2 μL of alkaline phosphatase (FastAP thermosensitive Alkaline phosphatase, New England Biolabs, Ipswich, USA) and 11 μL of buffer (10X FastAP Buffer, New England Biolabs, Ipswich, USA) were added in each Eppendorf tube. It remained at 37˚C for 25 minutes. 1 μL of EDTA was added to the sample and they were transferred at 60˚C for 20 minutes to deactivate the alkaline phosphatase enzyme.

3.1.4 DNA Purification

To allow a better ligation, all the enzymes and other products left in the sample must be removed. Therefore, a purification step was necessary. First, 300 μL of water and 400 μL of phenol were added in each sample. Samples were vortexed and centrifuged during 5 minutes at maximum speed (18000xg). The supernatant was mixed with 400 μL of Chloroform and centrifuged during 5 minutes at maximum speed (18000xg). The supernatant was mixed with 1000 μL of ethanol 100% and 40 μL of Sodium Acetate. Samples were kept in a freezer at -80˚C for 30 minutes. Then, they were centrifuged during 15 minutes at maximum speed (18000xg). The supernatant was discarded, and 300 μL of ethanol 70 % were added to the pellet. The samples were centrifuged during 5 minutes at maximum speed (18000xg). Once again, the supernatant was discarded, and the samples were dried in the SpeedVac (Savant^{TM} SpeedVac^{TM} High Capacity Concentrators, Thermo Fisher Scientific, Waltham, USA) during 5 to 9 minutes. DNA was resuspended in 12 μL of water.

3.1.5 DNA Ligation

For the ligation, the insert/vector ratio was 3 :1, i.e 6 μL of insert and 2 μL of vector were mixed with 2 μL of ligation buffer 10X (New England Biolabs, Ipswich, USA), 1,5 μL of ligase (New England Biolabs, Ipswich, USA) and 7,5 μL of water. Samples were incubated for 1 hour at room temperature or overnight at 16˚C.

3.1.6 Transformation in *Escherichia coli* (E. Coli)

10 μL of the ligation mix was added to 40 μL of bacteria E. Coli (*DH5α*). Samples were kept during 20 minutes on ice. A thermic choc at 42˚C for 45 seconds was performed to introduce the plasmid in the bacteria. Bacteria were plated on LB (Bacto-tryptone 1 %, Bacto-Yeast extract 0,5 %, NaCL 1 %) with Ampicillin (Sigma-Aldrich, Saint-Louis, USA) overnight. Recombinant colonies were amplified in 10 mL of LB and the plasmids were purified with the GeneJET Plasmid Miniprep Kit (Thermo Fisher Scientific, Waltham, USA) according to the manufacturer instructions.

3.1.7 Cloning verification

The presence in the plasmid of the cDNA of interest was assessed by PCR. Primers in **Table 3** were used for the screening. 23 colonies were screened for each construction.

3.1.8 Gel migration

After each PCR, the amplification product was loaded in a 1 % agarose gel and electrophoresis was performed during 20 minutes at 110 volts. This step was performed to assess the amplicons size. The gel was composed of 5g agarose, 500 mL of TAE and ethidium bromide (Carl Roth, Karlsruche, Germany). Detection on the gel was performed by an UV lamp (265 nm).

3.1.9 Mutation correction

Following sequencing of the constructs, the mutations identified in our constructs were corrected using the QuickChange II Site-Directed Mutagenesis Kit (Stratagene, San Diego, USA) according to the manufacturer recommendations.

3.2 Cell preparation for Nano Bioluminescence Resonance Energy Transfer (NanoBRET)

HEK293T cells were cultured with DMEM (Lonza, Bâle, Switzerland) supplemented with 10 % FBS (GE Healthcare Life Sciences, Issaquah, USA), 1 % Pen/Strep (Gibco, Carlsbad, USA) at 37˚C, 5 % CO_2 in T75 culture flask (Sigma-Aldrich, Saint-Louis, USA). Once they reached 70-90 % confluence, medium was removed and the cells were washed with 4 mL of Phosphate buffered saline (PBS). PBS was then discarded and 2 mL of trypsin-EDTA were added. Trypsin was neutralized with 8 mL medium and cells were counted using the Beckman Coulter Vi-Cell XR^{TM} (Analis, Namur, Belgium). $8{\cdot}10^5$ cells per well were seeded in a 6-well plate. Cells were incubated at 37˚C, 5 % CO_2 during 4 to 6 hours, to allow them to attach.

Transfection mix was prepared as follows. 1 μg of HaloTag fusion vector DNA (either tagged with ABCB5β, ABCB6 or ABCB9) and 1 μg of NanoLuc fusion vector DNA (either tag with ABCB5β, ABCB6 or ABCB9) were added to 200 μL of jetPRIME buffer (Polyplus transfection, Illkirch, France). 4 μL of jetPRIME (Polyplus transfection, Illkirch, France) were added andEppendorf were incubated at room temperature for 10 minutes. The mix was added to the cells, which were incubated at 37˚C, 5 % CO_2 for 24 hours. Medium was removed and cells were washed with 1 mL PBS. PBS was removed and 0,5 mL of trypsin-EDTA was added. 2 mL of medium were added to the well. Cells were harvested in 15 mL tubes, and were centrifuged at 125xg for 5 minutes. Medium was removed and cells were washed with 1 mL PBS followed by a centrifugation at 125xg for 5 minutes. PBS was removed and cells were resuspended in 2 mL of opti-MEM I reduced serum medium no phenol red (Gibco, Carlsbad, USA) supplemented with 4 % FBS (GE Healthcare Life Sciences, Issaquah, USA). Cells were counted using the Beckman Coulter Vi-Cell XR^{TM} (Analis, Namur, Belgium) and prepared to reach a density of $2 \cdot 10^5$ cells per mL.

Two different conditions were assessed. First, 1 μL of 0,1 mM HaloTag NanoBRET ligand 618 (NanoBRET^{TM} Protein: Protein interaction system, Promega, Madison, USA) per mL of cells were added. Second, 1 μL of Dimethyl sulfoxide (DMSO) per mL of cells were added. 100 μL of the mix, cells with ligand or DMSO, were plated in a 96-well plate and were cultured overnight at 37˚C 5 % CO2.

3.3 Nano Bioluminescence Resonance Energy Transfer (NanoBRET)

A mix with 2,5 mL of opti-MEM I reduced serum medium no phenol red (Gibco, Carlsbad, USA) and 25 μL of NanoBRET^{TM} NanoGlo® substrate (NanoBRET^{TM} Protein: Protein interaction system, Promega, Madison, USA) was prepared. The mix was added to the cells and the 96-well plate was shaken for 30 seconds. Within 10 minutes, donor emission (447 nm) and acceptor emission (610 nm) were measured using a dual filter (SpectraMax, Molecular Devices, San José, USA).

4 Results

Cloning of ABCB5*β*, ABCB6 and ABCB9 into HaloTag and NanoLuc plasmids

To validate the heterodimerization of ABCB5*β* with ABCB6 and ABCB9 using the NanoBRET system, ABCB5*β*, ABCB6 and ABCB9 had first to be cloned in NanoLuc (pNLF1N[CMV/Hygro] and pNLF1-C[CMV/Hygro]) and HaloTag (pHTC HaloTag CMV-neo and pHTN HaloTag CMV-neo) containing vectors. ABCB5*β*, ABCB6 and ABCB9 sequences were first amplified from plasmids available in the laboratory using polymerase chain reaction (PCR) with designed primers (**Table 3**). These primers were flanked with different restriction enzyme sites to allow the PCR products to be inserted into the plasmids (**Table 5**). Amplified PCR products were then digested and purified. Meanwhile, vectors were also digested, dephosphorylated and purified. After purification, the insert was ligated into the target vector using a 3:1 ratio. Constructs were then transformed into *E.Coli* (DH5*α*) and screened by PCR (**Figure 20**). Positive colonies were sent for sequencing.

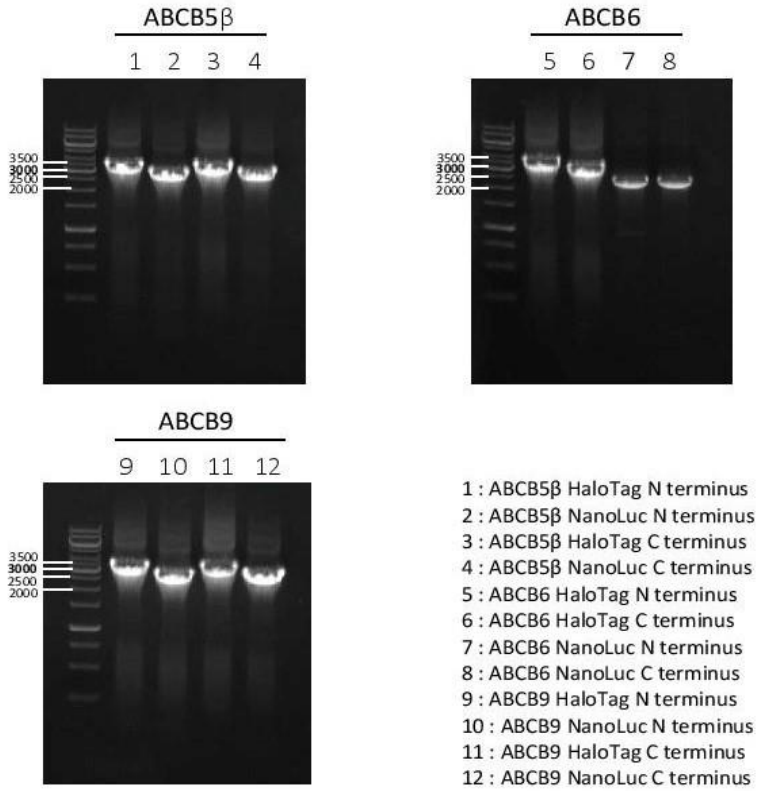

Figure 20 – Twelve constructs with ABCB5*β*, ABCB6 and ABCB9 in NanoLuc (pNLF1-N [CMV/Hygro] and pNLF1-C [CMV/Hygro]) and HaloTag (pHTN HaloTag CMV-neo and pHTN HaloTag CMV-neo) vectors. Regarding the ABCB5*β* constructs, a band is visible around 3500 bp (1), 3000 bp (2), 3500 bp (3) and 3000 bp (4). They all correspond to the amplification by PCR of the final product as the expected sizes are 3375 bp, 2979 bp, 3380 bp and 3015 bp, respectively. For the ABCB6 constructs, a band is visible around 3500 bp (5), 3500 bp (6), 3000 bp (7) and 3000 bp (8). They all correspond to the amplification by PCR of the final product as the expected sizes are 3465 bp, 3460 bp, 3069 bp and 3102 bp, respectively. For the ABCB9 constructs, a band is visible around 3500 bp (9), 3000 bp (10), 3500 bp (11) and 3000 bp (12). They all correspond to the amplification by PCR of the final product as the expected sizes are 3238 bp, 2841 bp, 3239 bp and 2874 bp, respectively.

It appeared that two out of the twelve constructs were carrying a mutation point (**Table 6**). ABCB6 cloned into the plasmid containing the sequence of NanoLuc in N terminus (pNLF1-N) exhibited an amino acid replacement, leading to the switch from a thymidine to a cysteine at the position 1914 of the cDNA (**Figure 21**). This mutation leads to the switch of a phenylalanine to a leucine between the Walker A and the Q loop. ABCB5*β*, also cloned into pNLF1-N, exhibited a mutation substituting a thymidine to an adenosine at the position 1006 from the start of the cDNA (**Figure 22**). This mutation leads to the change of an isoleucine to a phenylalanine in the cytosolic region between the second and the third *α*-helices of the transmembrane domain.

Plasmid	Mutation
ABCB6 NanoLuc N terminus	c.1914T>C
ABCB5*β* NanoLuc N terminus	c.1006T>A

Table 6 – Mutations in the final constructs.

Correction of mutation in pNLF1-N[CMV/Hygro] fused with ABCB6 and pNLF1N[CMV/Hygro] fused with ABCB5*β*

Two out of the twelve constructs engineered were carrying a mutation point (**Table 6**). Even though the mutations lead to the switch between two closely related amino acids at the protein level and might not disturb the conformation of the protein, it was decided to correct these mutations using site-directed mutagenesis. Primers were designed, and corrected plasmids were thenceforth amplified. Parental plasmids were next digested using DpnI enzyme, and resulting DNA was transformed into *E. Coli* (DH5*α*). Colonies were cultured the next day and sent for sequencing. Results showed that mutations were efficiently corrected (**Figure 21, 22**).

Figure 21 – Mutation correction of ABCB6 NanoLuc N terminus. A. Sequencing result showing mutation in ABCB6 NanoLuc N terminus leading in a change from a cysteine to a thymidine. A phenylalanine became a leucine between the Walker A and the Q loop. B. Sequencing result of ABCB6 NanoLuc N terminus corrected using QuickChange II SiteDirected Mutagenisis Kit.

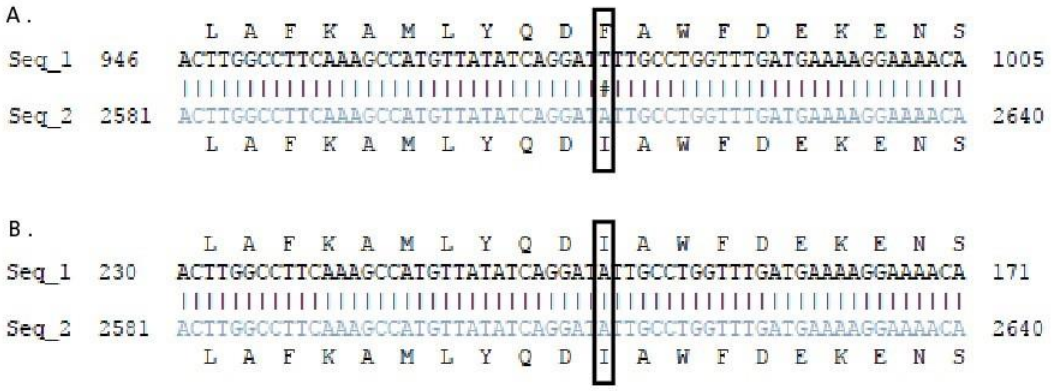

Figure 22 – Mutation correction of ABCB5*β* NanoLuc N terminus. A. Sequencing result showing mutation in ABCB5*β* NanoLuc N terminus leading in a change from a thymidine to an adenosine. An isoleucine became a phenylalanine in the cytosolic region between the second and the third *α*-helices of the transmembrane domain. B. Sequencing result of ABCB5*β* NanoLuc N terminus corrected using QuickChange II SiteDirected Mutagenisis Kit.

After the correction of the mutation, each construct was assessed by sequencing.

Nano Bioluminescence Resonance Energy Transfer of P53 and MDM2 as positive control

Twelve constructs were prepared, in which either ABCB6, ABCB9 or ABCB5*β* were inserted at the N- or C-terminal region of the HaloTag or NanoLuc. This allow us to test the homo- and heterodimerization of all the possible combinations between these three half-transporters using the NanoBRET system (**Annex 1)**. Each combination consists of a plasmid containing NanoLuc and another containing HaloTag. Before assessing the dimerization of ABCB5*β* with ABCB6 or ABCB9, we ran positive controls included in the kit (NanoBRET*™* Protein: Protein interaction system, Promega, Madison, USA) knowing NanoLuc®-MDM2 and p53-HaloTag® plasmids. MDM2 is the principal cellular antagonist of p53, it naturally suppresses the action of p53 in undamaged cells and has been shown to strongly interacts with p53 [60]. Plasmids were co-transfected in HEK293T cells, while a pool of cells was left untransfected. Cells were transferred in a 96-well plate, and NanoBRET HaloTag® 618 ligand was added to half of the wells, while DMSO was added to the other half as internal negative control. NanoBRET NanoGlo® substrate was next supplemented to all the wells and the plate was then read using SpectraMax (Molecular Devices, San José, USA) and a dual filter (Custom LUM type 660, Molecular Device, San José, USA) at 447 nm and 610 nm wavelengths.

Raw data were obtained and NanoBRET ratio, mean NanoBRET ratio and corrected ratio were alternately calculated (**Annex 2**). NanoBRET ratio is the the acceptor emission value (HaloTag), divided by the donor emission value (NanoLuc). Corrected ratio is the subtraction of NanoBRET ratio from samples without the ligand to NanoBRET ratio from samples with the ligand. Regarding transfected cells, donor emission values of wells with NanoBRET HaloTag® 618 ligand and in wells without it were closed (7 600 000 RLU with ligand and 8 200 000 RLU without, **Figure 23**). This was expected as they are both put in the presence of the substrate allowing NanoLuc to emit light at 447 nm. On the other hand, acceptor values were significantly higher in the samples with the ligand (495 000 RLU) than without it (70 500RLU) (**Figure 23**). This was expected, since the absence of the ligand prevents the samples to emit at 610 nm. Consequently, there were a significant difference in the NanoBRET ratio between samples with and without ligand. This led to a NanoBRET corrected ratio (NanoBRET ratio with the ligand - NanoBRET ratio with DMSO) of 56,4 mBU - milliBioluminescence Unit (**Figure 23**). This ratio was considered showing p53 and MDM2 interaction and thenceforward validating the method. For untransfected cells, a negative mean corrected ratio was measured. A negative value means that sample without the ligand had higher NanoBRET ratio than sample with the ligand. This shows the absence of HaloTag emission in these samples, resulting in the non-transfection of HaloTag and NanoLuc containing plasmids.

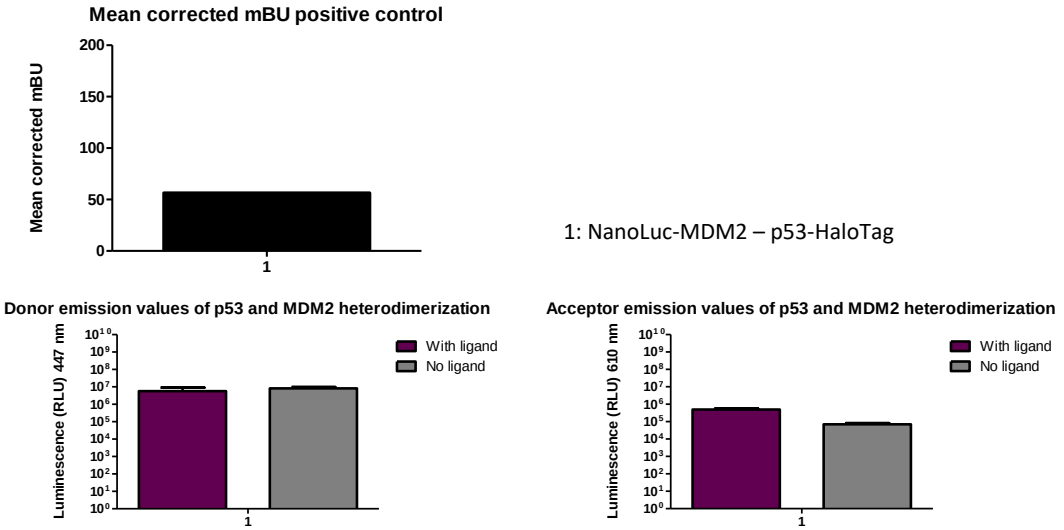

Figure 23 – HEK293T cells were transfected with NanoLuc®-MDM2 and p53-HaloTag®. Half of the wells were supplemented with NanoBRET HaloTag® 618 ligand. After, NanoBRET NanoGlo® substrate was added to all the conditions. Donor emission (emission of NanoLuc fused protein). Acceptor emission (emission of HaloTag fused protein) were obtained. Both donor emissions were quite similar and acceptor emission was higher in samples with the ligand. Then, NanoBRET ratio and mean corrected ratio were calculated using donor and acceptor emissions. The mean corrected ratio of 56.4 mBU showed p53 and MDM2 interaction as expected.

This experiment revealed that we were able to efficiently transfect p53-halotag fusion vector DNA and NanoLuc-MDM2 fusion vector DNA (NanoBRET*TM* Protein: Protein interaction system, Promega, Madison, USA) in HEK293T cells. Data were collected and showed the interaction of p53 and MDM2, confirming the efficiency of the method to highlight protein-protein interaction.

Nano Bioluminescence Resonance Energy Transfer of ABCB5*β* with p53 and MDM2 as negative control

Before analyzing ABCB5*β* heterodimerization with ABCB6 and ABCB9 using NanoBRET, a negative control of the method was performed. ABCB5*β* heterodimerization with p53 and MDM2 was assessed in HEK293T cells. Both p53 and MDM2, two soluble proteins, do not interact with ABCB5*β*, a membrane protein. MDM2 and p53 constructs provided by Promega were co-transfected with ABCB5*β* in HEK293T cells. All four possible combinations were assessed (**Figure 24**). After transfection, NanoBRET protocol was followed as previously described in the section describing the p53-MDM2 positive control experiments.

Raw data were obtained. NanoBRET ratio, mean NanoBRET ratio and corrected ratio were alternately calculated (**Annex 3**). NanoBRET ratio measured from samples with ligand were only on average 0,8-fold greater than the NanoBRET ratio in samples without ligand. Therefore, mean corrected mBU were respectively 2.8, 3.0, 1.4 and 2.4 for pair 1, 2, 3 and 4 (**Figure 24**). We decided to arbitrary define that a value above 10 highlighted the dimerization. None NanoBRET ratio value was greater than this threshold. This led us to determine that a ratio above that value was necessary to show an heterodimerization as no official threshold was determined, and all the NanoBRET experiments must include their own negative controls.

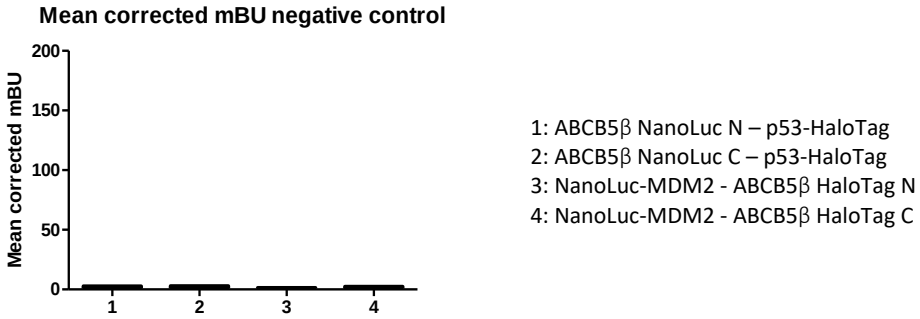

Figure 24 – HEK293T cells were transfected with four different combinations of constructs (1, 2, 3 and 4). Samples were supplemented with NanoBRET HaloTag® 618 ligand or DMSO. Then, NanoBRET NanoGlo® substrate was supplemented. After calculation, mean NanoBRET ratio was obtained. These ratios did not exceed 3 mBU. No interaction between ABCB5*β* with p53 or MDM2 was observed.

This experiment showed the absence of interaction between ABCB5*β* and p53 or MDM2. Ratio between cells with and without the NanoBRET HaloTag® 618 ligand didn't significantly increase. These results confirm the effectiveness of the technique and allow us to test the ABCB5*β* heterodimerization with other ABCB half-transporters.

Hetero- and homodimerization of ABCB5*β* with ABCB6 and ABCB9

The hetero- and homodimerization of ABCB5*β*, ABCB6 and ABCB9 were assessed in HEK293T cells with NanoBRET assay. As constructs were available, we decided to test ABCB6 and ABCB9 heterodimerization as well. Each DNA sequence was fused in N or C terminus of either HaloTag or NanoLuc-constructs (**Figure 19, 20**). Each vector combination to be tested were co-transfected in HEK293T cells (**Annex 1**). Experiments were run in triplicates.

Heterodimerization raw data were obtained. NanoBRET ratio, mean NanoBRET ratio and corrected ratio were calculated (**Annex 4**). Mean corrected ratio of each heterodimerization were plotted (**Figure 25**). ABCB5*β*/ABCB6 heterodimerization test showed high NanoBRET ratio for some combinations. Pair 1 (ABCB5*β* NanoLuc N terminus and ABCB6 HaloTag N terminus) reached the highest ratios with a corrected NanoBRET ratio of 88.5 mBU. This pair exhibits a NanoBRET ratio around twelve-foldgreater when ligand was added, compared to sample with DMSO (96.7 mBU against 8.2 mBU) (**Annex 4**). Other pairs, as pair 2, or to a lesser extend pair 5, also showed elevated NanoBRET ratios.

ABCB5*β*/ABCB9 heterodimerization test also revealed high NanoBRET ratio for some combinations (**Figure 25**). Pair 1 (ABCB5*β* NanoLuc N terminus and ABCB9 HaloTag N terminus) reached the highest ratios with a corrected NanoBRET ratio of 69.4 mBU. This pair displays a NanoBRET ratio around nine-fold greater when ligand was added, compared to sample with DMSO (77.8 mBU against 8.3 mBU) (**Annex 4**). Other pairs, as pair 2, or to a lesser extend pair 5, also showed elevated NanoBRET ratios.

ABCB6/ABCB9 heterodimerization test, like the previous ones, indicates high NanoBRET ratio for some combinations (**Figure 25**). Pair 1 (ABCB6 NanoLuc N terminus and ABCB9 HaloTag N terminus) reached the greatest ratios with a corrected NanoBRET ratio of 71.7 mBU. This pair has a NanoBRET ratio around nine-fold greater when ligand was added, compared to sample with DMSO (80.2 mBU against 8.6 mBU) (**Annex 4**). Other pairs, as pair 2 or 8, also showed elevated NanoBRET ratio.

a.

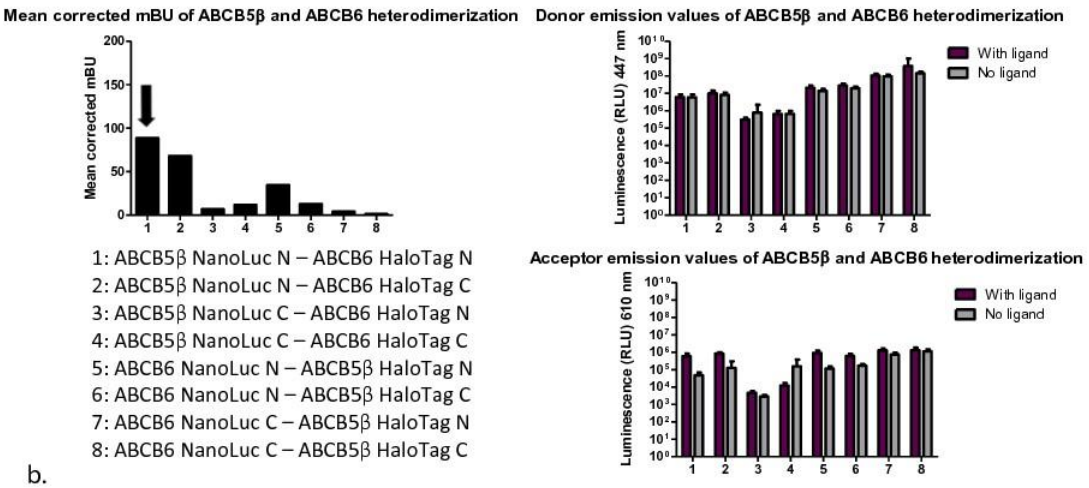

b.

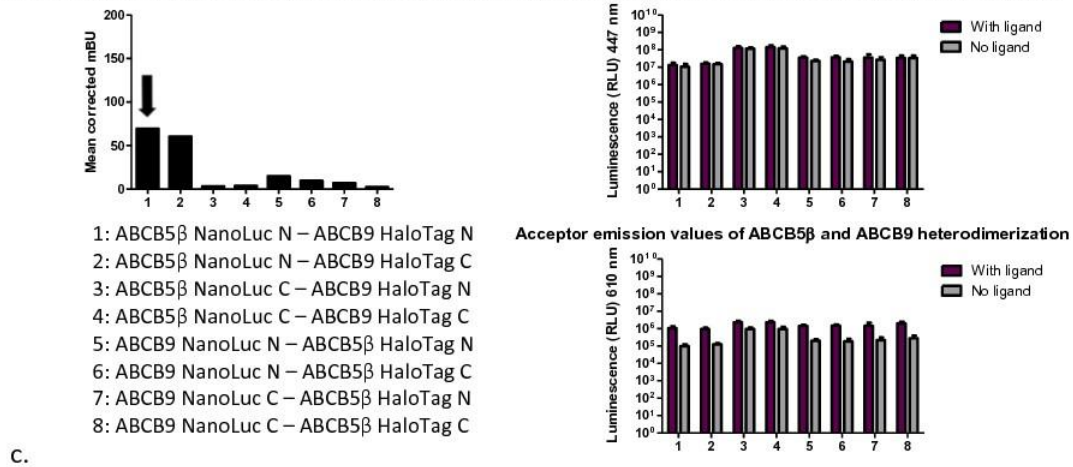

c.

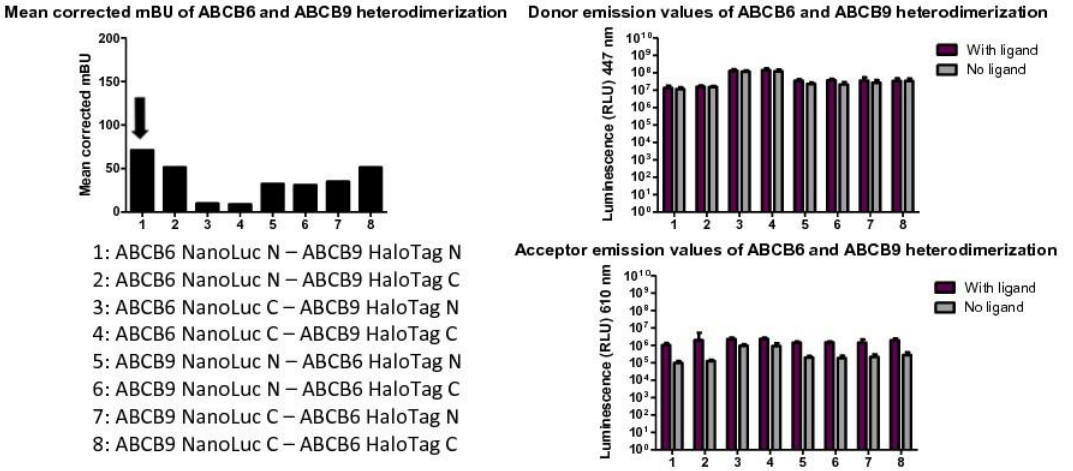

Figure 25 – Heterodimerizations of ABCB5*β* with ABCB6, ABCB5*β* with ABCB9 and ABCB6 with ABCB9 were investigated. Constructs were transfected in HEK293T cells. NanoBRET ligand and substrate were added. Fluorescence emission of the donor and acceptor were read at 447 nm and 610 nm wavelengths. NanoBRET ratio and mean corrected ratio were calculated. a. ABCB5*β* and ABCB6 heterodimerization yielded a mean corrected ratio of 96.7 mBU, 76.5 mBU and 42,7 mBU for its three best pairs, respectively 1, 2 and 5. b. ABCB5*β* and ABCB9 heterodimerization yielded a mean corrected ratio of 77.8 mBU, 68.5 mBU and 23.4 mBU for its three best pairs, respectively 1, 2 and 5. c. ABCB6 and ABCB9 heterodimerization yielded a mean corrected ratio of 80.2 mBU, 59.3 mBU and 59.2 mBU for its three best pairs, respectively 1, 2 and 8. Heterodimerization of ABCB5*β* with ABCB6, ABCB5*β* with ABCB9 and ABCB6 with ABCB9 has been successfully shown. A pair, marked with a black arrow, in each test was selected for further investigation depending on theNanoBRET ratio, donor emission and acceptor emission.

Afterwards, homodimerization raw data were obtained. NanoBRET ratio, mean NanoBRET ratio and corrected ratio were calculated (**Annex 6**). Mean corrected ratio of each homodimerization were plotted (**Figure 26**). ABCB5*β* homodimerization test showed high NanoBRET ratio for one combination. Pair 1 (ABCB5*β* NanoLuc N terminus and ABCB5*β* HaloTag N terminus) reached the highest ratio with a corrected NanoBRET ratio of 45.2 mBU. This pair exhibits a NanoBRET ratio around six-fold greater when ligand was added, compared to sample with DMSO (53.6 mBU against 8.4 mBU) (**Annex 6**). No other pair showed similar results.

ABCB6 homodimerization test also revealed high NanoBRET ratio for some combinations (**Figure 26**). This result was expected as ABCB6 homodimerization has already been highlighted in the literature [61]. Pair 4 (ABCB6 NanoLuc C terminus and ABCB6 HaloTag C terminus) reached the greatest ratios with a corrected NanoBRET ratio of 66.8 mBU. This pair displays a NanoBRET ratio around seven-fold greater when ligand was added, compared to sample with DMSO (74.9 mBU against 8.2 mBU) (**Annex 6**). Other pairs, pairs 1 and 2, also showed elevated NanoBRET ratios.

ABCB9 homodimerization test, like the previous ones, indicates high NanoBRET ratio for some combinations (**Figure 26**). Once again, this result was expected as ABCB9 homodimerization has already been highlighted in the literature [62]. Pair 4 (ABCB9 NanoLuc C terminus and ABCB9 HaloTag C) reached the highest ratios with a corrected NanoBRET ratio of 109.2 mBU. This pair has a NanoBRET ratio around fourteen-fold greater when ligand was added, compared to sample with DMSO (117.2 mBU against 8 mBU) (**Annex 6**). Pairs 1, 2 and 3 also showed high NanoBRET ratios.

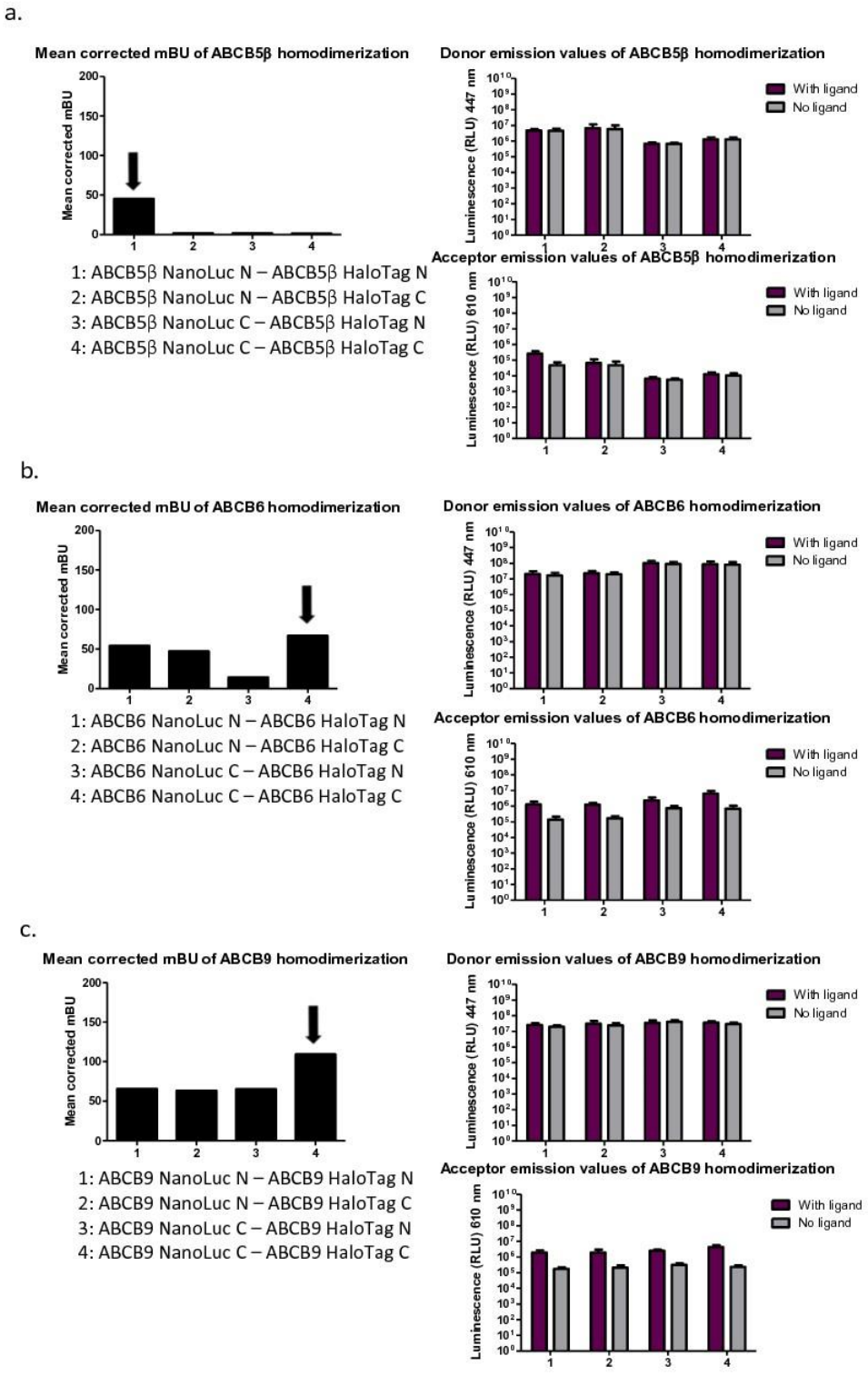

Figure 26 – Homodimerizations of ABCB5*β*, ABCB6 and ABCB9 were investigated. Constructs were transfected in HEK293T cells. NanoBRET ligand and substrate were added. Fluorescence emission of the donor and acceptor were read at 447 nm and 610 nm wavelength. NanoBRET ratios and mean corrected NanoBRET ratios were calculated. a. ABCB5*β* homodimerization yielded a mean corrected ratio of 53.6 mBU for the best pair, 1. b. ABCB6 homodimerization yielded a mean corrected ratio of 75 mBU for the best pair, 4. c. ABCB9 homodimerization yielded a mean corrected ratio of 117,2 mBU for the best pair, 4. Homodimerizations of ABCB5*β*, ABCB6 and ABCB9 have been successfully shown. A pair, marked with a black arrow, in each test was selected for further investigation depending on their NanoBRET ratio, donor emission and acceptor emission.

For each heterodimerization and homodimerization investigation, a pair has been chosen for further analysis based on its NanoBRET ratio, donor emission and acceptor emission values. To be selected, the pair had to present the higher NanoBRET ratio with a donor emission and acceptor emission values above 400 RLU. 400 was defined as threshold because during experiments, all the samples showing a value below 400 led to aberrant results underlining the limit of the fluorescence detection for the instrument. The six selected pairs are highlighted by a black arrow in **Figure 25 and 26**.

From a statistical point of view, ABCB5*β* with ABCB6, ABCB5*β* with ABCB9 and ABCB6 with ABCB9 heterodimerizations were significant as the difference between samples with the ligand and without ligand was prominent. We can draw the same conclusion for ABCB5*β*, ABCB6 and ABCB9 homodimerizations. Heterodimerizations were the most substantial with the pairs ABCB5*β* NanoLuc N terminus - ABCB6 HaloTag N terminus, ABCB5*β* NanoLuc N terminus - ABCB9 HaloTag N terminus and ABCB6 NanoLuc N terminus - ABCB9 HaloTag N terminus. Homodimerization was the most considerable with the pair ABCB5*β* NanoLuc N terminus - ABCB5*β* HaloTag N terminus, ABCB6 NanoLuc C terminus - ABCB6 HaloTag C terminus and ABCB9 NanoLuc C terminus - ABCB9 HaloTag C terminus. All of them were selected to undergo a donor dilution assay followed by a donor saturation assay.

Statistical analysis of ABCB5*β*, ABCB6 and ABCB9 hetero- and homodimerization

Heterodimerization and homodimerization data were obtained and analyzed. All the results were confirmed by statistical analysis. Samples without the ligand were used as an assay validity criterion but were not included in the statistical analysis. In fact, all the NanoBRET ratios varied around 8 and subtracted them to the ligand values wouldn't have any effect on the statistical conclusion as they were very consistent for each assay (**Annexes 4 and 6**). Moreover, each experiment contained three technical replicates and three biological replicates. As each technical replicates data were very close, they were employed as proof of adequate performance for each assay, but not as a relevant representation of the experimental variability. Mean of technical replicates was accordingly used. Experimental variability necessary to assess the significance of the effect factors was the variability between assays, biological replicates.

Three different effect factors were determined: position of the donor (Pos1), position of the acceptor (Pos2) and type of dimer (Di). Position of the donor could either be N terminus or C terminus (N or C, **Figure 27**), position of the acceptor could either be N terminus or C terminus (N or C, **Figure 28**) and type of dimer could be the donor fused with a protein and the acceptor with the next one or the opposite. For example, ABCB5*β* tagged with the donor and ABCB6 tagged with the acceptor or ABCB6 tagged with the donor and ABCB5*β* tagged with the acceptor (B-56 or B-65, **Figure 29**).

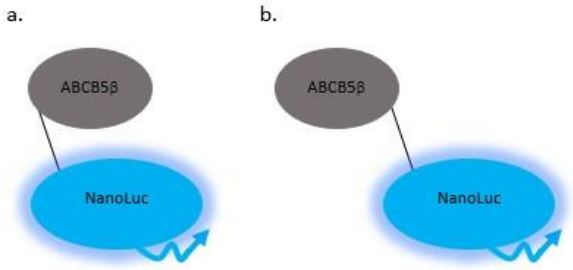

Figure 27 – Position of the donor, NanoLuc, can be N terminus (a) or C terminus (b) of the protein of interest represented here by ABCB5*β* here. Image derived from Figure 15.

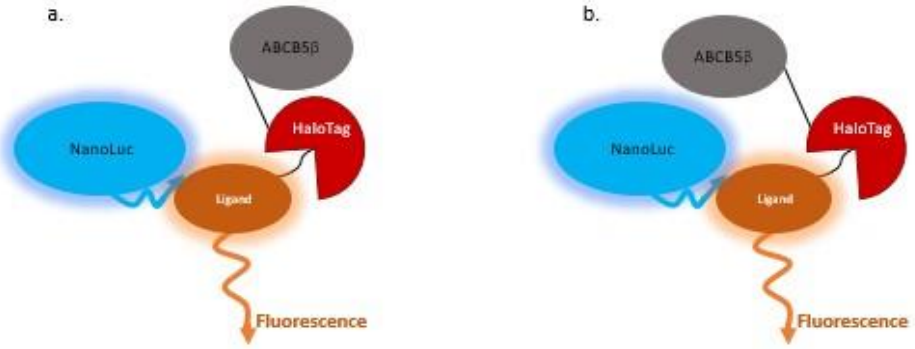

Figure 28 – Position of the acceptor, HaloTag, can be N terminus (a) or C terminus (b) of the protein of interest represented by here ABCB5*β* here. Image derived from Figure 15.

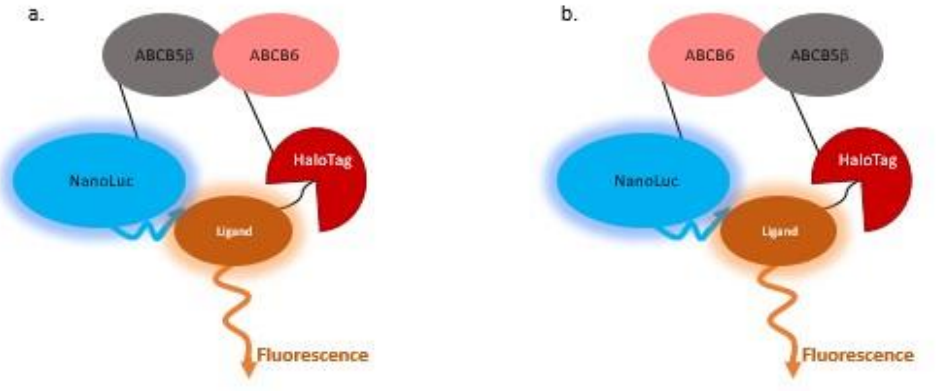

Figure 29 – Type of dimer can either be ABCB5*β* tagged with the donor and ABCB6 tagged with the acceptor (a) or ABCB6 tagged with the donor and ABCB5*β* tagged with the acceptor (b). a) ABCB5*β* NanoLuc N terminus and ABCB6 HaloTag N terminus heterodimerization (B-56). b) ABCB6 NanoLuc N terminus and ABCB5*β* HaloTag N terminus heterodimerization (B-65). Image derived from Figure 15.

A three-way fixed ANOVA has been performed on the R software for each heterodimerization investigation. Sum of square of the different factors has been plotted (**Figure 30 - 32**). Regarding ABCB5β and ABCB6 heterodimerization, P1 and Di showed a high contribution to the heterodimerization, 54% and 25%, respectively. Interaction plot leads to the conclusion that P1=N, P2=N and Di=B-56 should be preferred to obtain a higher mBU (**Annex 5**). Experimental error, corresponding to variability between biological replicates, was 2.9 mBU. For ABCB5β and ABCB9 heterodimerization, P1, Di and Di$*$P1 (the interaction between the position of the first tag and the type of tag) showed a high contribution to the heterodimerization, 44%, 24% and 26%, respectively. Interaction plot lead to the conclusion that P1=N, P2=N and Di=B-59 should be preferred to obtain a higher mBU (**Annex 5**). Experimental error was 7,0 mBU. Concerning ABCB6 and ABCB9 heterodimerization, P1 and Di$*$P1 showed a high contribution to the heterodimerization, 25% and 56%, respectively. Interaction plot leads to the conclusion that P1=N, P2=N and Di=B-69 should be preferred to obtain a higher mBU (**Annex 5**). Experimental error was 7,6 mBU.

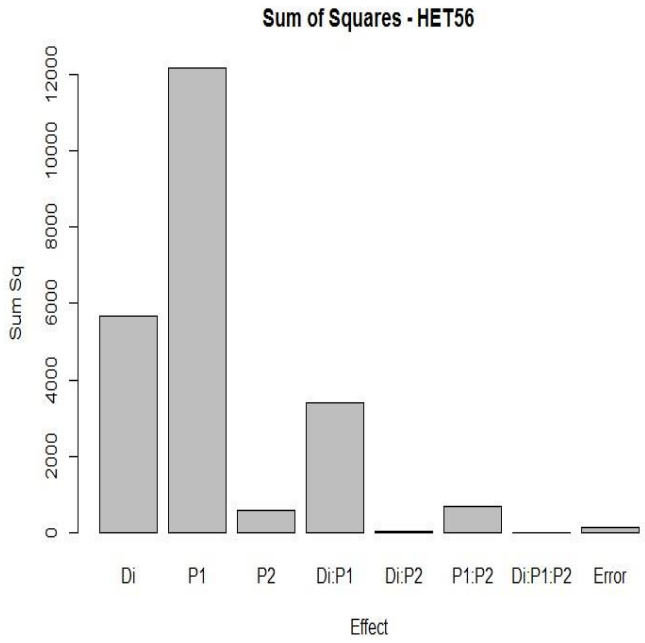

Figure 30 – Regarding ABCB5β heterodimerization with ABCB6, sum of square of each factor studied by ANOVA and interaction between factors were plotted. The sum of square indicates the variability for one factor. The greater it was the more variability regarding this point there was. Di is when ABCB5β is tagged with NanoLuc and ABCB6 tagged with HaloTag or ABCB6 tagged with NanoLuc and ABCB5β is tagged with HaloTag. P1 is the position of NanoLuc either in N or C terminus of the protein of interest. P2 is the position of HaloTag either in N or C terminus of the protein of interest. Di:P1 is the interaction between the type of dimer and the position of P1. Di:P2 is the interaction between the type of dimer and the position of P2. P1:P2 is the interaction between the position 1 and 2. Di:P1:P2 is the interaction between the three factors. Di and P1 were the two factors that influenced the most the ABCB5β and ABCB6 heterodimerization.

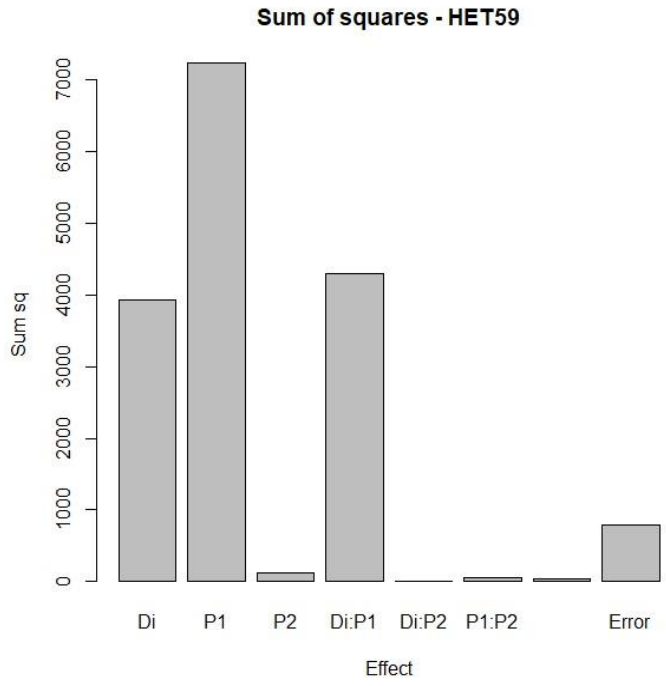

Figure 31 – Regarding ABCB5*β* heterodimerization with ABCB9, sum of square of each factor studied by ANOVA and interaction between factors was plotted. The sum of square indicates the variability for one factor. The greater it was the more variability regarding this point there was. Di is when ABCB5*β* is tagged with NanoLuc and ABCB9 tagged with HaloTag or ABCB9 tagged with NanoLuc and ABCB5*β* tagged with HaloTag. P1 is the position of NanoLuc either in N or C terminus of the protein of interest. P2 is the position of HaloTag either in N or C terminus of the protein of interest. Di:P1 is the interaction between the type of dimer and the position of P1. Di:P2 is the interaction between the type of dimer and the position of P2. P1:P2 is the interaction between the position 1 and 2. Di:P1:P2 is the interaction between the three factors. Di, P1 and Di:P1 were the three factors that influenced the most the ABCB5*β* and ABCB9 heterodimerization.

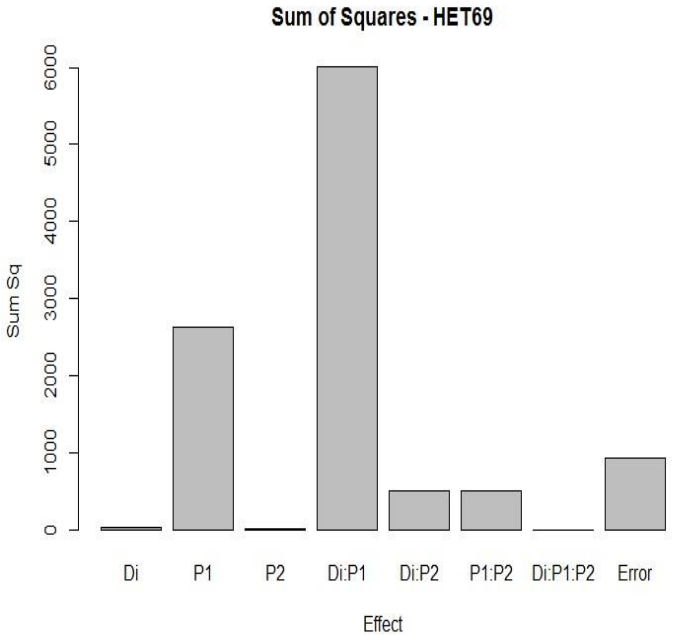

Figure 32 – Regarding ABCB6 heterodimerization with ABCB9, sum of square of each factor studied by ANOVA and interaction between factors was plotted. The sum of square indicates the variability for one factor. The greater it was the more variability regarding this point there was. Di is when ABCB6 is tagged with NanoLuc and ABCB9 tagged with HaloTag or ABCB9 tagged with NanoLuc and ABCB6 tagged with HaloTag. P1 is the position of NanoLuc either in N or C terminus of the protein of interest. P2 is the position of HaloTag either in N or C terminus of the protein of interest. Di:P1 is the interaction between the type of dimer and the position of P1. Di:P2 is the interaction between the type of dimer and the position of P2. P1:P2 is the interaction between the position 1 and 2. Di:P1:P2 is the interaction between the three factors. P1 and Di:P1 were the two factors that influenced the most the ABCB6 and ABCB9 heterodimerization.

Regarding the homodimerization, two different effect factors were determined: the position of the donor (Pos1) and the position of the acceptor (Pos2) (**Figure 27** and **Figure 28**). A two-way fixed ANOVA has been performed on the R software. Sum of square of the different factors has been plotted (**Figure 33 - 35**). Regarding the ABCB5β homodimerization, P1, P2 and P1$*$P2 (interaction between the position of the donor and the position of the acceptor) showed a high contribution to the homodimerization, 30%, 30% and 29%, respectively. We concluded that P1=N and P2=N should be preferred to obtain a higher mBU. Experimental error was 8.1 mBU. Concerning ABCB6 homodimerization, P2 and P1$*$P2 showed a high contribution to the homodimerization, 31% and 53%, respectively. We can conclude that P1=C and P2=C should be preferred to obtain a higher mBU. Experimental error was 8.2 mBU. For the ABCB9 homodimerization, P1 and P1$*$P2 showed a high contribution to the homodimerization, 36% and 31%, respectively. P1=C and P2=C should be preferred to obtain a higher mBU. Experimental error was 13.0 mBU.

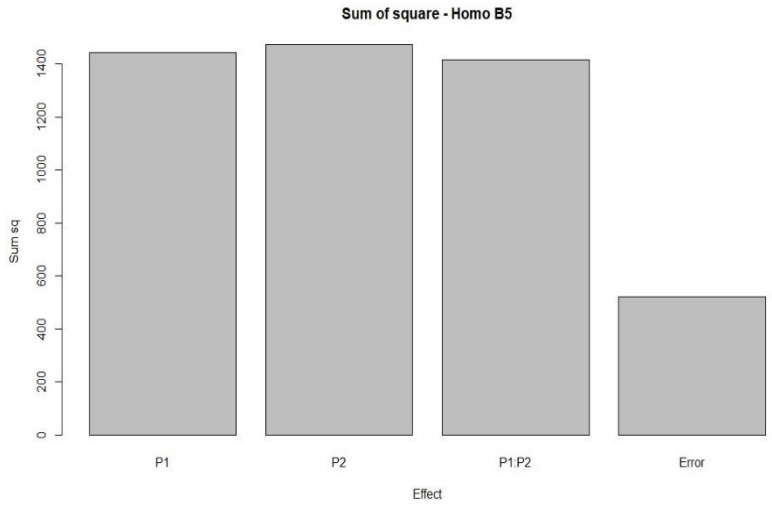

Figure 33 – Regarding ABCB5β homodimerization, sum of square of each factor studied by ANOVA and interaction between factors was plotted. The sum of square indicates the variability for one factor. The greater it was the more variability regarding this point there was. P1 is the position of NanoLuc either in N or C terminus of ABCB5β. P2 is the position of HaloTag either in N or C terminus of ABCB5β. P1:P2 is the interaction between the position 1 and 2. P1, P2 and P1:P2 were the three factors that influenced the most the ABCB5β homodimerization.

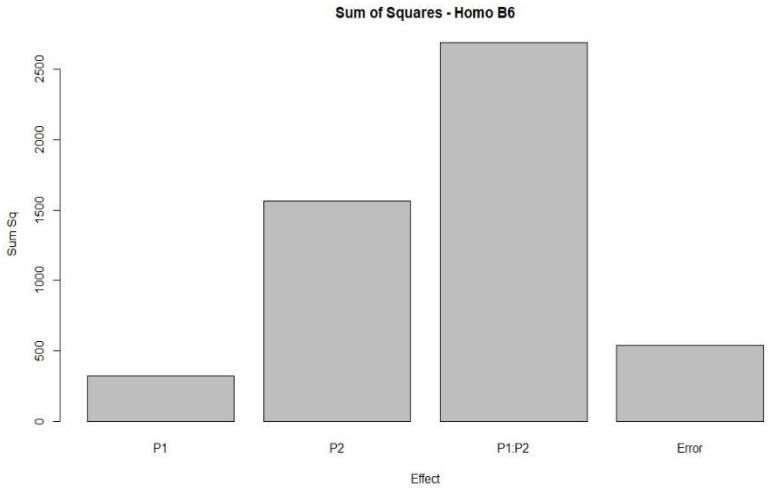

Figure 34 – Regarding ABCB6 homodimerization, sum of square of each factors studied by ANOVA and interaction between factor was plotted. The sum of square indicates the variability for one factor. The greater it was the more variability regarding this point there was. P1 is the position of NanoLuc either in N or C terminus of ABCB6. P2 is the position of HaloTag either in N or C terminus of ABCB6. P1:P2 is the interaction between the position 1 and 2. P1 and P1:P2 were the two factors that influenced the most the ABCB6 homodimerization.

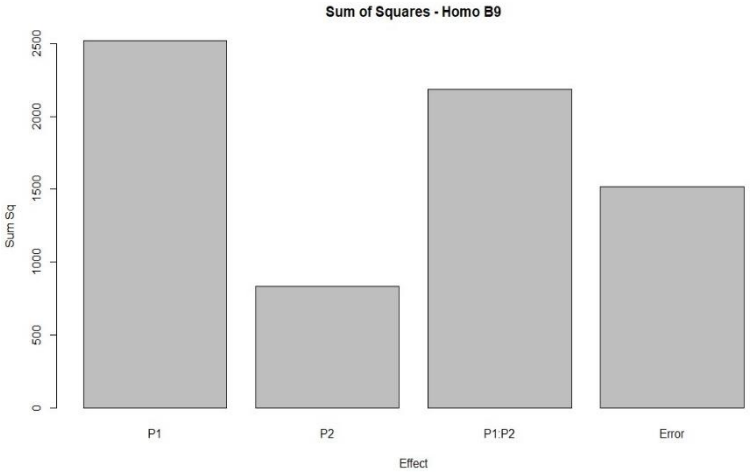

Figure 35 – Regarding ABCB9 homodimerization, sum of square of each factor studied by ANOVA and interaction between factors was plotted. The sum of square indicates the variability for one factor. The greater it was the more variability regarding this point there was. P1 is the position of NanoLuc either in N or C terminus of ABCB9. P2 is the position of HaloTag either in N or C terminus of ABCB9. P1:P2 is the interaction between the position 1 and 2. P1 and P1:P2 were the two factors that influenced the most the ABCB9 homodimerization.

Statistical analysis confirmed the choice of the selected pairs. Moreover, the variability remained below 13, which does not influence our results.

ABCB5β, ABCB6, ABCB9 hetero- and homodimerization donor dilution assay

After successful evidence of ABCB5β, ABCB6 and ABCB9 hetero- and homodimerization, each pair previously selected presenting the higher NanoBRET ratio, sufficient donor emission and acceptor emission underwent a donor dilution assay (**Figure 25 and 26**).

Donor dilution assay allowed to determine the donor concentration presenting the best dynamic range. Each pair was transfected in HEK293T cells following a decreasing amount of NanoLuc fused protein (i.e. 1 μg NanoLuc - 1 μg HaloTag, 0.2 μg NanoLuc - 2 μg HaloTag, 0.02 μg NanoLuc - 2 μg HaloTag and 0.002 μg NanoLuc - 2 μg HaloTag). Cells were transferred in a 96-well plate, and NanoBRET HaloTag® 618 ligand was added to half of the wells, while DMSO was added to the other half as negative control. NanoBRET NanoGlo® substrate was next added to all the wells and the plate was read using SpectraMax (Molecular Devices, San José, USA) and a dual filter (Custom LUM type 660, Molecular Device, San José, USA) at 447 nm and 610 nm wavelengths. For each combination, the experiment was repeated starting at the transfection two separate times. Raw data were obtained and the NanoBRET and mean NanoBRET ratios were calculated (**Annex 7**). 0.2 μg NanoLuc and 2 μg HaloTag corresponding to the ratio 1:10 has been chosen as optimal concentration for hetero- and homodimers. In fact, for most of the combinations it was the ratio showing the most important NanoBRET ratio, while maintaining donor and acceptor emission values broadly above the limit fluorescence detection for the instrument (**Annex 7**). This ratio was used to calculate the amount of HaloTag and NanoLuc fusion proteins to be transfected in the donor saturation assay.

ABCB5*β*, ABCB6, ABCB9 hetero- and homodimerization donor saturation assay

Successful donor dilution assay allowed us to determine the concentration where each selected pair highlighted the best NanoBRET ratio, while keeping an important donor and acceptor emission values. 1:10 ratio had been used to choose donor saturation assay concentration of NanoLuc and HaloTag.

Each selected pair had to pass a donor saturation assay to determine if the interaction highlighted was specific or not. In fact, each combination previously selected might exhibit an important NanoBRET ratio because both fluorophores were in close proximity due to over-expression of the fusion proteins, but without interacting with each other. To do so, decreasing concentration of HaloTag constructs were transfected in HEK293T cells, while identical concentration of NanoLuc constructs were transfected (**Table 2**). After, cells were transferred in a 96-well plate and NanoBRET HaloTag® 618 ligand was added to half of the wells, while DMSO was added to the other half as negative control. NanoBRET NanoGlo® substrate was next added to all the wells and plate was read using SpectraMax (Molecular Devices, San José, USA) and a dual filter (Custom LUM type 660, Molecular Device, San José, USA) at 447 nm and 610 nm wavelengths. For each combination, the experiment was done starting at the transfection three separate times. Results were plotted as percentage of maximum NanoBRET ratio in function of NanoLuc-HaloTag ratio transfected. For a growing amount of HaloTag fusion proteins, if the signal increased linearly, the NanoBRET result would be considered as non-specific (**Figure 16**). On the other hand, if signal increased in a hyperbolic way and reached a plateau, meaning that all donors were saturated with acceptor molecules, NanoBRET signal would be considered as specific (**Figure 16**).

An exception has been made for ABCB5*β* homodimerization. Even though the dilution assay gave identical results than for other homodimers, the ABCB5*β* donor saturation assay didn't show interpretable results for five different concentrations previously selected. Other ratios were defined (**Annex 8**).

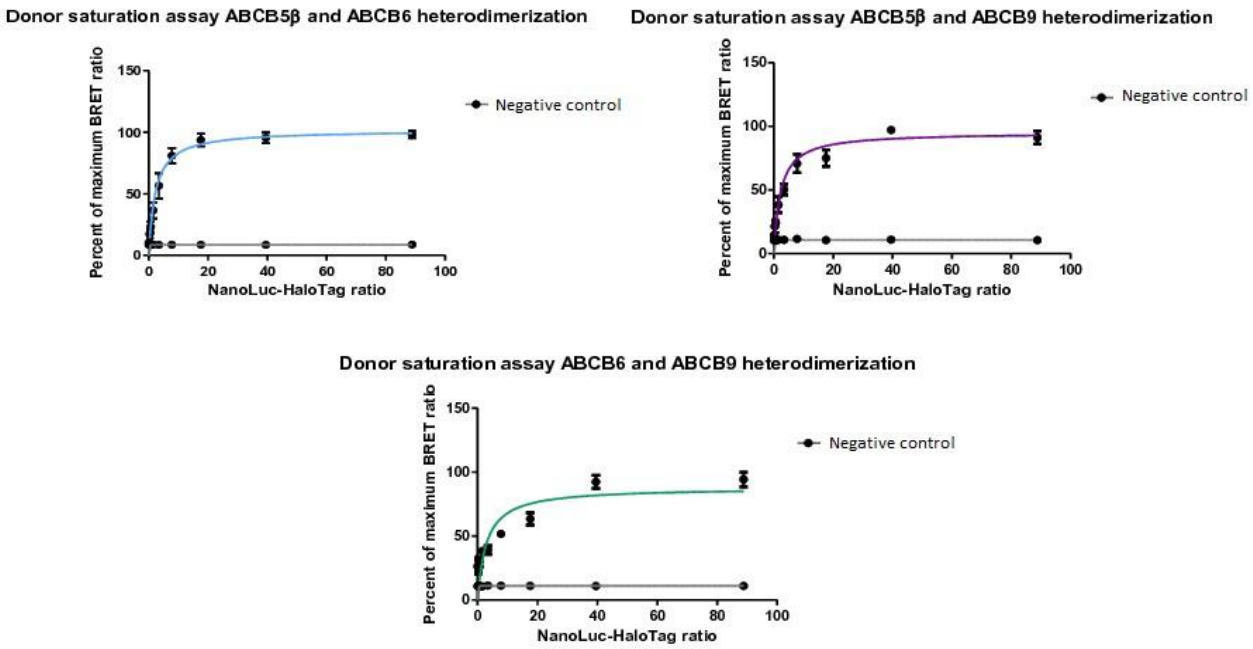

Figure 36 – Donor saturation assay of ABCB5*β* with ABCB6, ABCB5*β* with ABCB9 and ABCB6 with ABCB9 heterodimerization has been done. Nine different NanoLuc-HaloTag ratios were used (**Table 2**). Emissions were read at 447 nm and 610 nm. NanoBRET ratio was plotted as percent of maximum NanoBRET ratio in function of NanoLuc-HaloTag ratio transfected. Regarding ABCB5*β* with ABCB6, ABCB5*β* with ABCB9 and ABCB6 with ABCB9 heterodimerization, a hyperbolic curve was observed. It suggests NanoLuc fused proteins became saturated by the growing amount of HaloTag fused proteins showing a specific heterodimerization for each selected pair. The negative control was a technical negative control (sample without ligand and with DMSO).

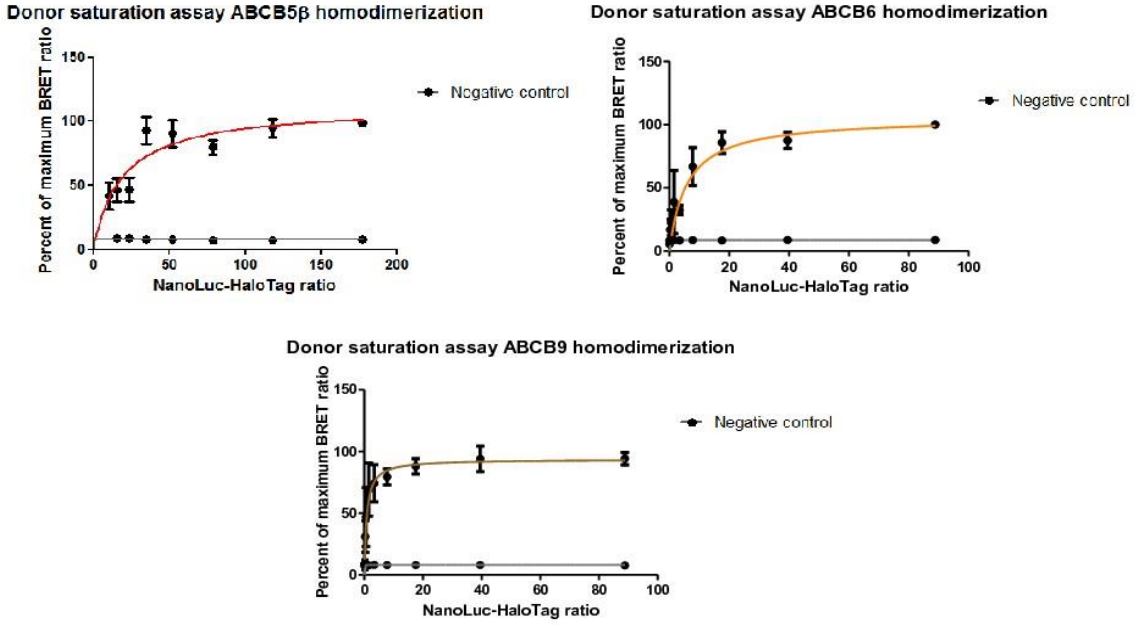

Figure 37 – Donor saturation assay of ABCB5*β*, ABCB6 and ABCB9 homodimerization has been done. Nine different NanoLuc-HaloTag ratios were used (**Table 2**) excepted for ABCB5*β* (**Annex 8**). Emissions were read at 447 nm and 610 nm. NanoBRET ratio was plotted as percent of maximum NanoBRET ratio in function of NanoLuc-HaloTag ratio transfected. Regarding ABCB5*β*, ABCB6 and ABCB9 homodimerization, a hyperbolic curve was observed. It was because NanoLuc fused proteins became saturated by the growing amount of HaloTag fused proteins showing a specific homodimerization for each selected pair. The negative control was a technical negative control (sample without ligand and with DMSO).

Each selected pair, heterodimers or homodimers, showed a hyperbolic signal (**Figure 36, 37**). It suggests that each NanoBRET experiment resulted in a specific interaction as the donor, fused with the protein of interest, was each time saturated with a growing number of acceptors fused with the protein of interest, resulting in a plateau (**Figure 36, 37**). These saturation curves (**Figure 36, 37**) confirm that each heterodimerization and homodimerization that we observed do not result from the over-expression of fusion proteins in HEK293T cells, but to the dimerization of these half-transporters.

5 Discussion and perspectives

ABCB5*β*, a member of the ATP-Binding Cassette transporter superfamily, is a half transporter potentially involved in chemoresistance in melanoma. This transporter is little characterized and information about its function are still unknown. Its potential dimerization has been proposed by *Lefèvre et al.* by co-immunoprecipitation of ABCB5*β* with ABCB6 and ABCB9 [44]. This master thesis aimed to validate these heterodimerizations. To do so, Nano Bioluminescence Resonance Energy Transfer (NanoBRET assay) has been chosen. It corresponds to a transfer of energy from a donor (NanoLuc) to an acceptor (HaloTag) when they are in close proximity. To perform the NanoBRET assay, ABCB5*β*, ABCB6 and ABCB9 were successfully cloned in NanoLuc and HaloTag plasmids. The heterodimerization of p53 with MDM2 and heterodimerization of ABCB5*β* with p53 or MDM2 were performed as positive and negative controls of the NanoBRET method, respectively. For the NanoBRET negative control, a similar NanoBRET ratio for samples with and without the ligand was shown. This highlight the lack of interaction between ABCB5*β* and p53 or MDM2. With regard to the positive control, the NanoBRET ratio in samples with the ligand was clearly above the NanoBRET ratio without the ligand, showing the interaction between p53 and MDM2. The negative and positive controls validated the method and allowed us to investigate ABCB5*β*, ABCB6 and ABCB9 dimerization. The corresponding DNA sequences tagged either with NanoLuc or HaloTag were transfected in HEK293T cells and all the possible homo- and heterodimerizations were investigated. For each assay, eight combinations of the different heterodimers and four combinations for the different homodimers were tested (**Annex 1**). Some NanoBRET ratios did stand out and a pair, in each experiment, has been selected (**Figure 25 and 26**). The selected pair had to show the best NanoBRET ratio, while maintaining a donor and acceptor emission values above the detection limit of the instrument.

Each selected pair underwent a donor dilution saturation assay. Donor dilution assay allowed to determine the concentration presenting the best dynamic range and has been used to optimize the donor saturation assay. Donor saturation assay allowed to define if the interaction between NanoLuc fused proteins and HaloTag fused proteins was specific or not. Each selected pair became saturated by the growing amount of acceptor leading to the conclusion that each interaction is specific and does not result from over-expression of proteins in cells. The results of the ABCB5*β* homodimerization donor saturation assay are an exception. The first donor saturation assay didn't show any interpretable results at the concentration used for the other homodimers. Concentrations needed to be increased and although we could generate a hyperbole-like curve for this homodimer, questions can be raised. The ABCB5*β* homodimer was expressed in High-5 insect cells to assess its basal ATPase activity. This latter was found to be much lower than the one of the typical ABCB5FL transporter [43]. Overall, this homodimer conformation could not be the preferential one for this transporter. Consequently, ABCB5*β* might during the experiment heterodimerize with other ABCB transporters expressed in HEK293T cells (e.g. ABCB6, ABCB9), decreasing possible interaction between NanoLuc and HaloTag. This hypothesis cannot be confirmed by the NanoBRET assay. In conclusion, experiments revealed that ABCB5*β* heterodimerizes with ABCB6 and ABCB9, ABCB6 heterodimerizes with ABCB9. The study also revealed the homodimerization of ABCB5*β*, ABCB6 and ABCB9.

Dimerization could have been studied by different methods (i.e. Chromatography, tandem affinity purification, phage display, chemical cross-linking, microscale thermophoresis, BioID, APEX, NanoBIT, Fluorescence Resonance Energy Transfer, etc.) [53] [55] [63]. For example, protein-fragment complementation assay (PCA) is commonly used to characterize protein-protein interaction. It is an enzyme or a fluorescent protein divided in two fragments. Each fragment is fused separately to proteins of interest. When both proteins are close from one another, each fragment previously divided interacts, resulting in the restored function visible by fluorescence or enzyme activity [64]. This technique is highly sensitive but is capable to detect interactions in a large perimeter [64]. Thereof, NanoBRET has been considered as a first choice experiment to investigate protein-protein interactions. Indeed, NanoBRET is easily implemented, relatively inexpensive and presents little drawbacks. Because NanoBRET signal could occur only when NanoLuc and HaloTag are closer than 10 nm, hetero- and homodimerization could easily be highlighted and false positive susceptibility is decreased [55]. Moreover, it is a highly sensitive method and it yields high performances [55].

When analyzing the NanoBRET ratios, some point out radically. For example, ABCB9 homodimerization highest ratio was 129 mBU, while ABCB5β homodimerization highest ratio was 70 mBU. One could conclude that ABCB9 homodimerizes more substantially than ABCB5β, but such a conclusion cannot be made. Indeed, too much variables are coming into account. Therefore, intensity of NanoBRET assay with different proteins cannot be compared between them. The most important variable is the tag orientation. It is important to know that an absence of signal does not mean absence of interaction. This affirmation challenges our negative control however, p53 and ABCB5β are two unrelated proteins. The first one is soluble and regulates cell cycle, autophagy and apoptosis. This protein becomes active in damaged cells and is known as the "guardian of the genome" [65]. The second one is a membrane protein and aims to transport different substrates [39]. Even if ABCB5β seems to play a role in cancer development, its interaction seems very unlikely. Nevertheless, another negative control is required to strengthen our results. The NanoBRET assay analyzing the interaction of ABCD3 with ABCB5β could be performed. Indeed, ABCD3 is a half transporter of the ABCD family and its heterodimerization with ABCD1 has already been highlighted by FRET [25]. Its interaction with a member of another family, ABCB family, is not expected. Likewise, ABCB9 heterodimerization with ABCB3 or ABCB2 could be used as negative control. Leverson-Gower *et al.* already claimed that these two half ABCB transporters did not heterodimerize together after dihydrofolate reductase protein-fragment complementation assay (DHFR-PCA) [62].

Evidence of ABCB6 and ABCB9 homodimerization correlates with literature. Leverson-Gower *et al.* found evidence of ABCB9 homodimerization thanks to DHFR-PCA [62]. Their first intention was to demonstrate the heterodimerization of ABCB9 with ABCB2 and ABCB3, two endoplasmic reticulum transporters known to dimerize together. The rationale of this study was that these three transporters share more than 30% amino acid sequence identity. As mentioned above, absence of heterodimerization between ABCB9 and one of these half transporters has been concluded [62]. On the other hand, ABCB9 homodimerization has been demonstrated [62]. Furthermore, Krishnamurthy *et al.* demonstrated by coimmunoprecipitation that ABCB6 homodimerizes in NIH3T3 cells [61]. It reinforces our results also exhibiting ABCB9 and ABCB6 homodimerizations.

ABCB6 localization has been hypothesized to vary upon cell type [66]. ABCB6 traffics to the endoplasmic reticulum and is, there, glycosylated depending on the cell type [66]. This glycosylation is suspected to influence ABCB6 trafficking. It results in different organelle localization based on the glycosylation and to some extend to the cell type [66]. As it seems possible for the ABCB transporters to be expressed in different locations depending on the cell type, hetero- or homodimerization could occur only in certain cells or tissues. Beforehand, heterodimerization of different zinc transporters has shown a different subcellular localization than homodimers [67]. Their heterodimerization altered localization of these transporters resulting in a possible change in the molecular mechanisms [67]. Subcellular localization of the heterodimers revealed in the current study should be assessed. Moreover, it is not excluded that ABCB5*β*/ABCB6 or ABCB5*β*/ABCB9 heterodimers transport different substrates than the ABCB5*β* homodimer or the ABCB5FL. Cytotoxic assays or transport assays should contribute to answer these questions.

ABCB6 and ABCB9 heterodimerization reinforce previous publications about their localization. In fact, both half-transporters have been shown to be localized in the lysosome [27] [34]. Moreover, in our laboratory, Guerit and colleagues confirmed these results using de Duve fractionation as they found that both transporters are expressed in the fraction L accountable for the lysosomal enriched fraction [68].

ABCB5*β* possible dimerization motifs were proposed by Moitra, *et al*. Bioinformatics have shown coiled-coil structures in the N terminus region of ABCB5*β* [38]. These structures are two *α*-helices pack together, usually involved in protein-protein interaction [38]. The hypothesis around this discovery is that ABCB5*β* dimerizes thanks to its coiled-coil domains. It strengthens our ABCB5*β* hetero- and homodimerization validation. An important step forward will be to expand Moitra, *et al*. results by investigating these dimerization processes and discovering how ABCB transporters interact together. Is there a heterodimerization motif in these ABCB transporters? Bioinformatic comparison of each ABCB transporter and crystallography will inform us on possible dimerization site.

Currently in our laboratory, ABCB5*β*, ABCB6 and ABCB9 heterodimerization with ABCB8 is being investigated. Preliminary results show that these half-transporters interact with ABCB8. Consequently, it is not excluded that most ABCB half-transporters heterodimerize together. Further investigations are needed and all half ABCB transporters (e.g. ABCB2, ABCB3, ABCB5*β*, ABCB6, ABCB7, ABCB8, ABCB9 and ABCB10) need to be tested for potential heterodimerization.

6 Conclusion

The objective of this master thesis was to validate the heterodimerization of ABCB5*β* with ABCB6 and ABCB9. Data showed that ABCB5*β* heterodimerizes with ABCB6 and ABCB9. Furthermore, we also highlighted the homodimerization of ABCB5*β*, ABCB6 and ABCB9 and the heterodimerization of ABCB6 with ABCB9.

This study contributed to bring a new set of data in the field of ABC transporters. It revealed four new ABC transporters knowing (ABCB5*β*-ABCB6, ABCB5*β*-ABCB9, ABCB6-ABCB9, and ABCB5*β* homodimer). This opens new perspectives for the investigation of the localization and the roles of these transporters in the cell.

References

[1] A. Shain and B. Bastian. From melanocytes to melanomas. *Nature Review Cancer*, 2016, 16(6), pp.345-358.

[2] B. Bastian. The molecular pathology of melanoma: an integrated taxonomy of melanocytic neoplasia. *Annu Rev Pathol*, 2016, pp.239-271.

[3] J. Thompson, R. Scolyer, and R. Kefford. Cutaneous melanoma. *The lancet*, 2005, 365(9460), pp.687-701.

[4] M. Situm, M. Buljan, M. Kolic, and M. Vucic. Melanoma-clinical, dermatoscopical, and histopathological morphological characteristics. *Acta Dermatovenerol Croat*, 2014, 22(1), pp.1-12.

[5] X. Liu and M. Saeed Sheikh. Melanoma: Molecular pathogenesis and therapeutic management. *Mol Cell Pharmacol*, 2014, 6(3), pp.228.

[6] A. Kyrgidis. Melanoma epidemiology. *Cutaneous melanoma: A pocket guide for diagnosis and management*, 2017, pp.1-9.

[7] J. Ferlay, I. Soerjomataram, R. Dikshit, S. Eser, C. Mathers, M. Rebelo, D. Parkin, D. Froman, and B. Freddie. Cancer incidence and mortality worldwide: Sources, methods and major patterns in globocan 2012. *Internatinal Journal of Cancer*, 2015, 136(5), pp.359-86.

[8] N. Matthews, W. Li, A. Qureshi, M. Weinstock, and E. Cho. Chapter 1: Epidemiology of melanoma. *Cutaneous melanoma: Etiology and therapy*, 2017.

[9] E. Erdei and S. Torres. A new understanding in the epidemiology of melanoma. *Expert Rev Anticancer Ther.*, 2010, 10(11), pp.1811-1823.

[10] P. Corrie, M. Hategan, K. Fife, and C. Parkinson. Management of melanoma. *British Medical Bulletin*, 2014, pp.149-162.

[11] KG. Chen, JC. Valencia, JP. Gillet, VJ. Hearing, and MM. Gottesman. Involvement of abc transporters in melanogenesis and the development of multidrug resistance of melanoma. *Pigment Cell Melanoma Res*, 2009, 22(6), pp.740-9.

[12] AS. Yang and Chapman PB. The history and futur of chemotherapy for melanoma. *Hematol Oncol Clin North Am*, 2010, pp.583-597.

[13] S. Rosenberg and M. Dudley. Adoptive cell therapy for the treatment of patients with metastatic melanoma. *Curr Opin Immunol*, 2009, 21(2), pp.233-240.

[14] L. Gatti and F. Zunino. Overview of tumor cell chemoresistance mechanisms. *Methods Mol Med*, 2005, pp.127-148.

[15] H. Zheng. The molecular mechanisms of chemoresistance in cancers. *Oncotarget*, 2017, 8(35), pp.59950-59964.

[16] M. Gottesman, O. Lavi, M. Hall, and JP. Gillet. Toward a better understanding of the complexity of cancer drug resistance. *Annual Review of Pharmacology and Toxicology*, 2016.

[17] Y. Sun, A. Patel, P. Kumar, and Z. Chen. Role of abc transporters in cancer chemotherapy. *Chin J Cancer*, 2012, 31(2), pp.51-57.

[18] J. Fletcher, M. Haber, M. Henderson, and M. Norris. Abc transporters in cancer: more than just drug efflux pumps. *Nature Reviews Cancer*, 2010, 10(2), pp.147-156.

[19] S. Heimerl, A. Bosserhoff, T. Langmann, J. Ecker, and G. Schmitz. Mapping atp-binding cassette transporter gene expression profiles in melanocytes and melanoma cells. *Melanoma Res.*, 2007, 17(5), pp.265-273.

[20] K. Chen, J. Valencia, B. Lai, G. Zhang, J. Paterson, F; Rouzaud, W. Berens, S. Wincovitch, S. Garfield, R. Leapman, V. Hearing, and M. Gottesman. Melanosomal sequestration of cytotoxic drugs contributes to the intractability of malignant melanomas. *pnas*, 2006, 103(26), pp.9903-9907.

[21] V. Vasiliou, K. Vasiliou, and D. Nebert. Human atp-binding cassette (abc) transporter family. *Human Genomics*, 3(3), p.281.

[22] D. Rees, E. Johnson, and O. Lewinson. Abc transporters: the power to change. *Nature Reviews Molecular Cell Biology*, 10(3), pp.218-227.

[23] D. Wanke and H. Uner Kolukisaoglu. An update on the abcc transporter family in plants: many genes, many proteins, but how many functions? *Plant biology*, 2010, 12, pp.15-25.

[24] N. Singh. Molecular modelling of human multidrug resistance protein 5 (abcc5). *Journal of Biophysical Chemistry*, 2016, 7(3), pp.61-73.

[25] M. Hillebrand, S. Verrier, A. Ohlenbush, A. Schafer, Soling H., F. Wouters, and J. Gartner. Live cell fret microscopy. *Journal of Biological Chemistry*, 282(37), pp.26997-27005.

[26] B. Erdelyi-Belle. Characterization of hepatocytes-like cells differentiated from human embryonic stem cell lines. *PhD thesis, Eotvos Lorand university, Faculty of Science*, 2015.

[27] J. Stefkova, R. Poledne, and J. Hubacek. Atp-binding cassette (abc) transporters in human metabolism and diseases. *Physiol. Res*, 2004, pp.235-243.

[28] M. Gottesman and S. Ambudkar. Overview: Abc transporters and human disease. *Journal of Bionergetics and Biomembranes*, 2001.

[29] T. Schatton, G. Murphy, N. Frank, K. Yamaura, A. Waaga-Gasser, M. Gasser, Q. Zhan, S. Jordan, L. Duncan, C. Weishaupt, R. Fuhlbridgge, T. Kupper, M. Sayegh, and M. Frank. Identification of cells initiating human melanomas. *Nature*, 2008, 451(7176), pp.345-349.

[30] R. Begicevic and M. Falasca. Abc transporters in cancer stem cells: Beyond chemoresistance. *Int J Mol Sci*, 2017, 18(11).

[31] T. Kawanobe, S. Kogure, S. Nakamura, S. Mai, K. Katayama, J. Mitsuhashi, K. Noguchi, and Y. Sugimoto. Expression of human abcb5 confers resistance to taxanes and anthracyclines. *Biochemical and biophysical research communications*, 2012, 418(4), pp.736-741.

[32] M. Herget and R. Tampé. Intracellular peptide transporters in human - compartmentalization of the peptidome. *Eur J Physiol*, 2007, 453, pp.591-600.

[33] Y. Zhao, M. Ishigami, K. Nagao, N. Kono, H. Arai, M. Matsuo, N. Kioka, and K. Ueda. Abcb4 exports phosphatidylcholine in a sphingomyelin-dependant manner. *J Lipid Res*, 2015, 56(3), pp.644-52.

[34] P. Bergam, J. Reisecker, Z. Rakvacs, N. Kucsma, G. Raposo, G. Szakacs, and G. Van Niel. Abcb6 resides in melanosomes and regulates early steps of melanogenesis required for pmel amyloid matrix formation. *Journal of Molecular Biology*, 2018.

[35] C. Pondarré, B. Antiochos, D. Campagna, S. Clarke, E. Greer, K. Deck, A. McDonald, A. Han, A. Medlock, J. Kutok, S. Anderson, R. Eisenstein, and M. Fleming. The

mitochondrial atp-binding cassette transporter abcb7 is essential in mice and participates in cytosolic iron - sulfur cluster biogenesis. *Human molecular genetics*, 2006, pp.953-964.

[36] M. Liesa, W. Qiu, and OS. Shirihai. Mitochondrial abc transporters function: the role of abcb10 (abc-me) as a novel player in cellular handling of reactive oxygen species. *Biochim Biophys Acta*, 2012, 1823(10), pp.1945-57.

[37] F. Zhang, W. Zhang, L. Liu, C. Fisher, D. Hui, S. Childs, K. Dorovini-zis, and V. Ling. Characterization of abcb9, an atp binding cassette protein associated with lysosomes. *Journal of Biological Chemistry*, 2000, 275, pp.233287-23294.

[38] K. Moitra, M. Scally, K. McGee, G. Lancaster, B. Gold, and M. Dean. Molecular evolutionary analysis of abcb5 : The ancestral gene is a full transporter with potentially deleterious single nucleotide polymorphisms. *PLoS One*, 2011, 6(1).

[39] S. Wang, L. Tang, J. Lin, Z. Shen, Y. Yao, W. Wang, S. Tao, C. Gu, J. Ma, Y. Xie, and Y. Liu. Abcb5 promotes melanoma metastasis through enhancing nf-kb p65 protein stability. *Biochemical and Biophysical Research*, 2017, pp.18-26.

[40] G. Sana, J. Madigan, J. Gartner, and al. et. Exome sequencing of abcb5 identifies recurrent melanoma mutations that result in increased proliferative and invasive capacities. *In final review*.

[41] K. Chen, G. Szakacs, JP. Annereau, F. Rouzaud, X. Liang, J. Valencia, C. Nagineni, J. Hooks, V. Hearing, and M. Gottesman. Principal expression of two mrna isoforms (abcb5alpha and abcb5beta) of the atp-binding cassette transporter gene abcb5 in melanoma cells and melanocytes. *Pigment cell res*, 2005, 18(2), pp.102-112.

[42] J. Lin, M. Zhang, T. Schatton, BJ Wilson, A. Alloo, J. Ma, A. Qureshi, Frank N., J. Han, and M. Frank. Genetically determined abcb5 functionality correlates with pigmentation phenotype and melanoma risk. *Biochem Biophys Res Commun*, 2013, 436(3), pp.536-542.

[43] M. Keniya, Holmes A., M. Niimi, E. Lamping, JP. Gillet, M. Gottesman, and R. Cannon. Drug resistance is conferred on the model yeast saccharomyces cerevisiae by expression of full-lenght melanoma-associated human atp-binding cassette transporter abcb5. *Molecular Pharmaceutics*, 2014, 11(10), pp.3452-3462.

[44] S. Lefèvre. Co-immunoprecipitation revealed the heterodimerization of the melanoma-associated abcb5 transporter with abcb6 and abcb9. Set up of a high five insect cells expression model to determine their physiological substrates. *Mémoire présenté pour l'obtention du grade académique de master en science biomédicales sous la direction de Jean-Pierre Gillet, Namur, Université de Namur*, 2018.

[45] H. Liu, Y. Li, K. Hung, N. Wang, C. Wang, X. Chen, D. Sheng, X. Fu, K. See, J. Foo, H. Low, H. Liany, I. Irwan, J. Liu, B. Yang, M. Chen, Y. Yu, G. Yu, G. Niu, C. Yuanhua, S. Chen, Q. Lieu, J. Liu, and F. Zhang. Genome-wide linkage, exome sequencing and functional analyses identify abcb6 as the pathogenic gene of dyschromatosis universalis hereditaria. *PLoS ONE*, 2014, 9(2).

[46] D. Piston and G. Kremers. Fluorescent protein fret: the good, the bad ans the ugly. *TRENDS in Biochemical Sciences*, 2007, 32(9).

[47] EA. Jares-Erijman and TM. Jovin. Fret imaging. *Nature Biotechnology*, 2003, 21(11), pp.1387-95.

[48] Northwestern University. Forster resonance energy transfer. *https*: *//cam.facilities.northwestern.edu/*588 − 2*/fluorescence − resonance − energy − transfer/*, On line.

[49] C. Dinant, M. Van Royen, W. Vermeulen, and A. Houtsmuller. Fluorescence resonance energy transfer of gfp and yfp by spectral imaging and quantitative acceptor photobleaching. *Journal of microscopy*, 2008.

[50] K. Pfleger and K. Eidne. Illuminating insights into protein-protein interactions using bioluminescence resonance energy transfer (bret). *Nature Methods*, 2006, 3(3), pp.165-174.

[51] A. Gorokhovatsky, V. Marchenkov, N. Rudenko, T. Ivashina, V. Ksenzenko, N. Burkhardt, G. Semisotnov, L. Vinokurov, and Y. Alakhov. Fusion of aequoarea victoria gfp and aequorin provides their ca2+-induced interaction that results in red shift of gfp absorption and efficient bioluminescence energy transfer. *Biochemical and Biophysical Research Communications*, 2004, 320(3), pp.703-711.

[52] A. Dragulescu-Andrasi, C. Chan, A. De, and S. Gambhir. Bioluminescence resonance energy transfer (bret) imaging of protein-protein interactions within deep tissues of living subjects. *Proceeding of the National Academy of Sciences of the United State of America*, 2011, 108(29), pp.12060-12065.

[53] S. Dimri and A. Basu, S. ans De. Use of bret to study protein-protein interactions in vitro and in vivo. *Methods Mol Biol*, 2016, pp.57-78.

[54] Promega. Nanobret protein: Protein interaction system. *Techincal Manual; instructions for use of the products*, N1661, N1662 and N1663.

[55] T. Machleidt, C. Woodroofe, M. Schwinn, J. Mendez, M. Robers, K. Zimmerman, P. Otto, D. Daniels, T. Kirkland, and K. Wood. Nanobret: A novel bret platform for the analysis of protein-protein interaction. *ACS Chem Biol*, 2015, 10(8), pp.1797-1804.

[56] L. Stoddart, E. Johnstone, A. Wheal, J. Goulding, M. Robers, T. Machleidt, K. Wood, S. Hill, and K. Pfleger. Application of bret to monitor ligand binding to gpcrs. *Nature Methods*, 2015, 12(7), pp.661-663.

[57] M. Hall, J. Unch, and K. Wood. Engineered luciferase reporter from a deep-sea shrimp utilizing a novel imidazopyrazinone substrate. *ACS Chemical Biology*, 2012, 7(11), pp.18481857.

[58] C. England, H. Luo, and W Cai. Halotag technology: A versatile platform for biomedical applications. *Bioconjugate Chemistry*, 2015, 26(6), pp.975-986.

[59] R. Mitchel. The bystander effect: recent developments and implications for understanding. *Nonlineary in biology, toxicology, medicine*, 2004, 2(3).

[60] U. Moll and O. Petrenko. The mdm2-p53 interaction. *Molecular cancer research*, 2003, 1, pp.1001-1008.

[61] P. Krishnamurthy, G. DU, Y. Fukuda, D. Sun, J. Sampath, K. Mercer, J. Wang, B. Sosapineda, G. Murti, and J. Schuetz. Identification of a mammalian mitochondrial porphyrin transporter. *Nature*, 2006.

[62] D. Leveson-Gower, S. Michnick, and V. Ling. Detection of tap family dimerization by an in vivo assay in mammalian cells. *Biochemistry*, 2004, 43, pp.14257-14264.

[63] Q. Chu, A. Rathore, J. Diedrich, C. Donaldson, J. Yates, and A. Saghatelian. Identification of microprotein-protein interactions via apex tagging. *Biochemistry*, 2017, 56(26), pp.32993306.

[64] E. Barnard and D. Timson. Detection of protein-protein interaction using protein-fragment complementation assays (pca). *Current proteomics*, 2007.

[65] S. Niazi, M. Purohit, and JH. Niazi. Pole of p53 circuitry in tumorigenesis: A brief review. *Eur J Med Chem*, 2018.

[66] Y. Fukuda, L. Aguilar-Bryan, M. Vaxillaire, A. Dechaume, Y. Wang, M. BEan, K. Moitra, J. Bryan, and J. Schuetz. Conserved intramolecular disulfide bond is critical to trafficking and fate of atp-binding cassette (abc) transporters abcb6 and sulfonylurea receptor 1 (sur1)/abcc8. *J Biol Chem*, 2011.

[67] Y. Golan, B. Berman, and Y. Assaraf. Heterodimerization, altered subcellular localization, and function of multiple zinc transporters in viable cells using bimolecular fluorescence complementation. *J Biol Chem*, 2015.

[68] E. Guérit. Generation of an ABCB5-knockout human melanoma cell line using the CRISPR/Cas9 genome editing-tool - Study of ABCB5 subcellular localization by cell fractionation. *Mémoire présenté pour l'obtention du grade académique de master en science biomédicales sous la direction de Jean-Pierre Gillet, Namur, Université de Namur*, 2019.

Annexes

Annex 1: Combinations of generated constructs to be tested in HEK293T cells

ABCB5β NanoLuc N terminus	ABCB6 HaloTag N terminus
ABCB5β NanoLuc N terminus	ABCB6 HaloTag C terminus
ABCB5β NanoLuc C terminus	ABCB6 HaloTag N terminus
ABCB5β NanoLuc C terminus	ABCB6 HaloTag C terminus
ABCB6 NanoLuc N terminus	ABCB5β HaloTag N terminus
ABCB6 NanoLuc N terminus	ABCB5β HaloTag C terminus
ABCB6 NanoLuc C terminus	ABCB5β HaloTag N terminus
ABCB6 NanoLuc C terminus	ABCB5β HaloTag C terminus

ABCB5β NanoLuc N terminus	ABCB9 HaloTag N terminus
ABCB5β NanoLuc N terminus	ABCB9 HaloTag C terminus
ABCB5β NanoLuc C terminus	ABCB9 HaloTag N terminus
ABCB5β NanoLuc C terminus	ABCB9 HaloTag C terminus
ABCB9 NanoLuc N terminus	ABCB5β HaloTag N terminus
ABCB9 NanoLuc N terminus	ABCB5β HaloTag C terminus
ABCB9 NanoLuc C terminus	ABCB5β HaloTag N terminus
ABCB9 NanoLuc C terminus	ABCB5β HaloTag C terminus

ABCB6 NanoLuc N terminus	ABCB9 HaloTag N terminus
ABCB6 NanoLuc N terminus	ABCB9 HaloTag C terminus
ABCB6 NanoLuc C terminus	ABCB9 HaloTag N terminus
ABCB6 NanoLuc C terminus	ABCB9 HaloTag C terminus
ABCB9 NanoLuc N terminus	ABCB6 HaloTag N terminus
ABCB9 NanoLuc N terminus	ABCB6 HaloTag C terminus
ABCB9 NanoLuc C terminus	ABCB6 HaloTag N terminus
ABCB9 NanoLuc C terminus	ABCB6 HaloTag C terminus

ABCB5β NanoLuc N terminus	ABCB5β HaloTag N terminus
ABCB5β NanoLuc N terminus	ABCB5β HaloTag C terminus
ABCB5β NanoLuc C terminus	ABCB5β HaloTag N terminus
ABCB5β NanoLuc C terminus	ABCB5β HaloTag C terminus

ABCB6 NanoLuc N terminus	ABCB6 HaloTag N terminus
ABCB6 NanoLuc N terminus	ABCB6 HaloTag C terminus
ABCB6 NanoLuc C terminus	ABCB6 HaloTag N terminus
ABCB6 NanoLuc C terminus	ABCB6 HaloTag C terminus

ABCB9 NanoLuc N terminus	ABCB9 HaloTag N terminus
ABCB9 NanoLuc N terminus	ABCB9 HaloTag C terminus
ABCB9 NanoLuc C terminus	ABCB9 HaloTag N terminus
ABCB9 NanoLuc C terminus	ABCB9 HaloTag C terminus

Annex 2: Positive control, p53 and MDM2 heterodimerization

NanoBRET ratio (mBU)		1	2	3	4 (mBU)	Mean NanoBRET ratio
Transfected cells	With ligand	66	62	66	65	64,8
	No ligand	8,8	8,5	7,5	8,8	8,4
Non-transfected cells	With ligand	180	120	140	260	175
	No ligand	310	200	330	160	250

Mean corrected ratio transfected cells: 56,4 mBU

Mean corrected ratio non-transfected cells: -75,00 mBU

Annex 3: Negative control, ABCB5β with p53 or MDM2 heterodimerization

NanoBRET ratio (mBU)	With ligand			No ligand		
B5β Nano N – p53 Halo	9	10	11	8	7	7
B5β Nano C – p53 Halo	11	12	11	8	9	9
Nano MDM2 - B5β Halo N	10	9	11	9	8	8
Nano MDM2 - B5β Halo C	11	11	10	9	8	8
B5β Nano N – p53 Halo	11	11	10	7	8	8
B5β Nano C – p53 Halo	11	11	11	8	7	8
Nano MDM2 - B5β Halo N	10	9	10	8	8	9
Nano MDM2 - B5β Halo C	9	10	10	8	7	8

Mean corrected ratio:

B5β Nano N – p53 Halo: 2,8 mBU

B5β Nano C – p53 Halo: 3,0 mBU

Nano MDM2 - B5β Halo N: 1,4 mBU

Nano MDM2 - B5β Halo C: 2 4 mBU

Annex 4: ABCB5β, ABCB6 and ABCB9 heterodimerization data

NanoBRET ratio (mBU)	With ligand			No ligand		
B5β Nano N – B6 Halo N	100	100	100	9	8	8
B5β Nano N – B6 Halo C	80	70	80	9	9	8
B5β Nano C – B6 Halo N	20	20	10	8	10	9
B5β Nano C – B6 Halo C	20	20	30	8	9	9
B6 Nano N - B5β Halo N	40	40	40	8	8	7
B6 Nano N - B5β Halo C	20	20	20	8	8	8
B6 Nano C - B5β Halo N	12	12	12	8	8	8
B6 Nano C - B5β Halo C	9	9	9	7	7	8
B5β Nano N – B6 Halo N	93	90	91	8	8	8
B5β Nano N – B6 Halo C	70	74	71	8	8	8
B5β Nano C – B6 Halo N	14	17	15	8	10	10
B5β Nano C – B6 Halo C	19	21	21	8	9	9
B6 Nano N - B5β Halo N	43	42	42	8	8	9
B6 Nano N - B5β Halo C	21	21	22	8	9	9
B6 Nano C - B5β Halo N	12	13	13	8	8	8

B6 Nano C - B5β Halo C	9	9	9	9	8	8
B5β Nano N – B6 Halo N	98	99	99	9	8	8
B5β Nano N – B6 Halo C	82	81	80	9	8	8
B5β Nano C – B6 Halo N	14	15	15	7	7	8
B5β Nano C – B6 Halo C	16	18	15	7	7	8
B6 Nano N - B5β Halo N	45	44	48	8	8	9
B6 Nano N - B5β Halo C	22	23	23	9	9	9
B6 Nano C - B5β Halo N	12	12	12	8	8	8
B6 Nano C - B5β Halo C	10	10	10	9	8	8

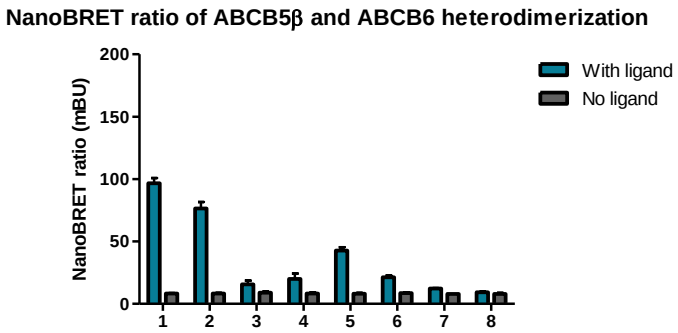

Mean corrected ratio:

B5β Nano N – B6 Halo N: 88,5 mBU

B5β Nano N – B6 Halo C: 68,1 mBU

B5β Nano C – B6 Halo N: 6,9 mBU

B5β Nano C – B6 Halo C: 11,8 mBU

B6 Nano N - B5β Halo N: 34,6 mBU

B6 Nano N - B5β Halo C: 12,9 mBU

B6 Nano C - B5β Halo N: 4,0 mBU

B6 Nano C - B5β Halo C: 1,3 mBU

NanoBRET ratio (mBU)	With ligand			No ligand		
B5β Nano N – B9 Halo N	77	88	90	8	8	8
B5β Nano N – B9 Halo C	88	88	91	8	8	7
B5β Nano C – B9 Halo N	10	11	10	7	8	8
B5β Nano C – B9 Halo C	10	10	12	8	9	7
B9 Nano N - B5β Halo N	23	23	23	8	8	8
B9 Nano N - B5β Halo C	16	16	15	8	8	8
B9 Nano C - B5β Halo N	16	16	14	8	8	8
B9 Nano C - B5β Halo C	10	10	10	8	8	8
B5β Nano N – B9 Halo N	79	79	77	9	8	8
B5β Nano N – B9 Halo C	61	61	62	8	8	8
B5β Nano C – B9 Halo N	11	10	10	8	8	8
B5β Nano C – B9 Halo C	15	12	12	9	9	8
B9 Nano N - B5β Halo N	23	23	24	9	9	9
B9 Nano N - B5β Halo C	19	20	19	9	9	9
B9 Nano C - B5β Halo N	16	18	19	8	8	8
B9 Nano C - B5β Halo C	11	12	10	9	8	8
B5β Nano N – B9 Halo N	71	69	70	8	9	9
B5β Nano N – B9 Halo C	56	58	52	8	10	8
B5β Nano C – B9 Halo N	12	13	12	8	8	8
B5β Nano C – B9 Halo C	14	14	12	10	9	8
B9 Nano N - B5β Halo N	26	25	21	9	9	9
B9 Nano N - B5β Halo C	19	20	19	9	8	9
B9 Nano C - B5β Halo N	12	12	13	8	9	9
B9 Nano C - B5β Halo C	11	10	11	9	8	8

NanoBRET ratio of ABCB5β and ABCB9 heterodimerization

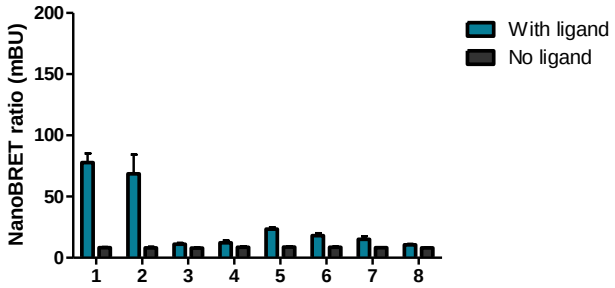

Mean corrected ratio:

B5β Nano N – B9 Halo N: 69,4 mBU

B5β Nano N – B9 Halo C: 60,4 mBU

B5β Nano C – B9 Halo N: 3,1 mBU

B5β Nano C – B9 Halo C: 3,8 mBU

B9 Nano N - B5β Halo N: 14,8 mBU

B9 Nano N - B5β Halo C: 9,6 mBU

B9 Nano C - B5β Halo N: 6,9 mBU

B9 Nano C - B5β Halo C: 2,4 mBU

NanoBRET ratio (mBU)	With ligand			No ligand		
B6 Nano N – B9 Halo N	71	71	67	9	9	9
B6 Nano N – B9 Halo C	53	49	46	8	9	8
B6 Nano C – B9 Halo N	17	17	16	8	8	8
B6 Nano C – B9 Halo C	16	15	15	8	8	8
B9 Nano N – B6 Halo N	38	36	40	9	9	10
B9 Nano N – B6 Halo C	36	36	36	9	9	10
B9 Nano C – B6 Halo N	49	47	38	8	9	9
B9 Nano C – B6 Halo C	53	52	48	8	8	8
B6 Nano N – B9 Halo N	87	86	87	9	8	8
B6 Nano N – B9 Halo C	71	69	73	8	8	8
B6 Nano C – B9 Halo N	17	19	17	8	8	8
B6 Nano C – B9 Halo C	18	19	20	8	8	8
B9 Nano N – B6 Halo N	39	42	36	9	8	8
B9 Nano N – B6 Halo C	42	43	41	10	10	8
B9 Nano C – B6 Halo N	30	31	30	8	8	8
B9 Nano C – B6 Halo C	58	56	58	8	8	8
B6 Nano N – B9 Halo N	81	87	85	8	9	8
B6 Nano N – B9 Halo C	58	56	59	8	8	8
B6 Nano C – B9 Halo N	20	19	17	8	8	8
B6 Nano C – B9 Halo C	19	16	13	8	8	8
B9 Nano N – B6 Halo N	47	45	45	8	8	8
B9 Nano N – B6 Halo C	41	41	44	8	8	8
B9 Nano C – B6 Halo N	62	44	57	8	8	8
B9 Nano C – B6 Halo C	70	67	71	8	8	8

NanoBRET ratio of ABCB6 and ABCB9 heterodimerization

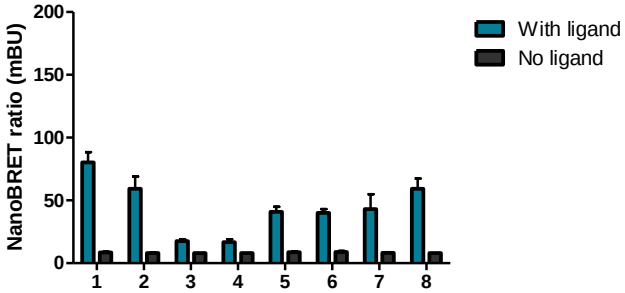

Mean corrected ratio:

B6 Nano N – B9 Halo N: 71,7 mBU

B6 Nano N – B9 Halo C: 51,2 mBU

B6 Nano C – B9 Halo N: 9,7 mBU

B6 Nano C – B9 Halo C: 8,8 mBU

B9 Nano N – B6 Halo N: 32,2 mBU

B9 Nano N – B6 Halo C: 31,1 mBU

B9 Nano C – B6 Halo N: 34,9 mBU

B9 Nano C – B6 Halo C: 51,2 mBU

Annex 5: ABCB5β, ABCB6 and ABCB9 heterodimerization interaction plot

Interaction plot of ABCB5β and ABCB6 heterodimerization (HET56) when P2=N or C:

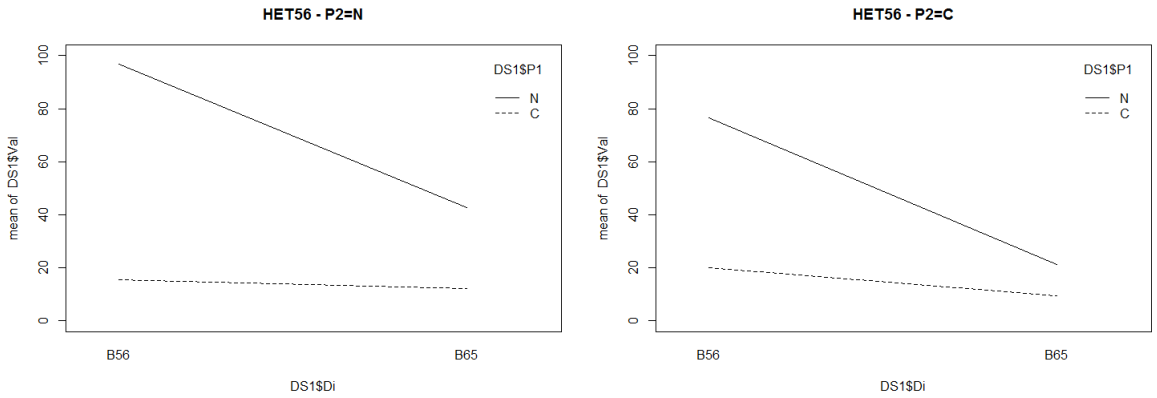

It's clearly visible that P1=C is suboptimal. P1=N results in a significant increase in response especially when the dimer is ABCB5β tagged with the donor and ABCB6 tagged with the acceptor (B56). P2 position doesn't really affect the trend as both interaction plot remain quite similar but P2=N should be preferred to obtain a higher mBU.

Interaction plot of ABCB5β and ABCB9 heterodimerization (HET59) when P2=N or C:

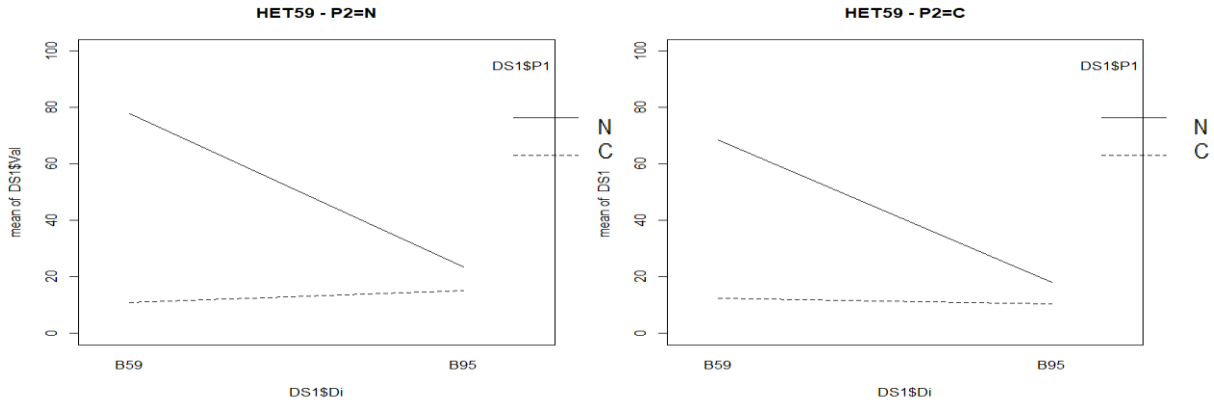

It's clearly visible that P1=C is suboptimal. P1=N results in a significant increase in response when the dimer is ABCB5β tagged with the donor and ABCB9 tagged with the acceptor (B59). P2 position doesn't really affect the trend as both interaction plot remain quite similar but P2=N should be preferred to obtain a higher mBU.

Interaction plot of ABCB6 and ABCB9 heterodimerization (HET69) when P2=N or C:

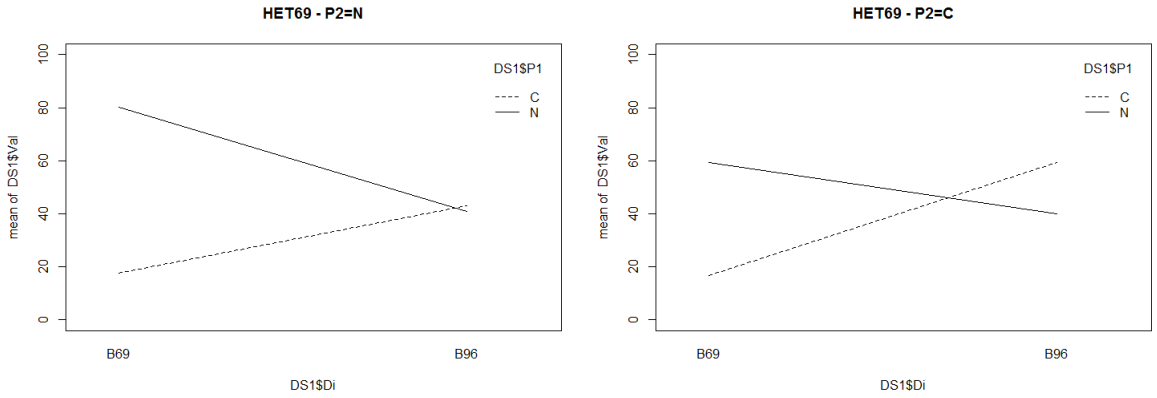

P1=C results in a significant increase in response when the dimer is ABCB9 tagged with the donor and ABCB6 tagged with the donor (B96). P1=N results in a significant increase in response when the dimer is ABCB6 tagged with the donor and ABCB9 tagged with the acceptor (B69). P2=N will be chosen to obtain a higher mBU.

Annex 6: ABCB5β, ABCB6 and ABCB9 homodimerization data

NanoBRET ratio (mBU)	With ligand			No ligand		
B5β Nano N – B5β Halo N	70	67	64	8	8	12
B5β Nano N – B5β Halo C	10	9	10	8	8	8
B5β Nano C – B5β Halo N	10	10	11	8	9	9
B5β Nano C – B5β Halo C	9	9	9	9	9	8
B5β Nano N – B5β Halo N	32	37	38	8	8	8
B5β Nano N – B5β Halo C	9	10	9	8	8	8
B5β Nano C – B5β Halo N	9	11	10	9	8	8
B5β Nano C – B5β Halo C	9	9	10	8	8	8
B5β Nano N – B5β Halo N	59	57	58	8	8	8
B5β Nano N – B5β Halo C	10	10	10	8	8	8
B5β Nano C – B5β Halo N	9	9	10	8	8	8
B5β Nano C – B5β Halo C	10	10	10	8	8	8

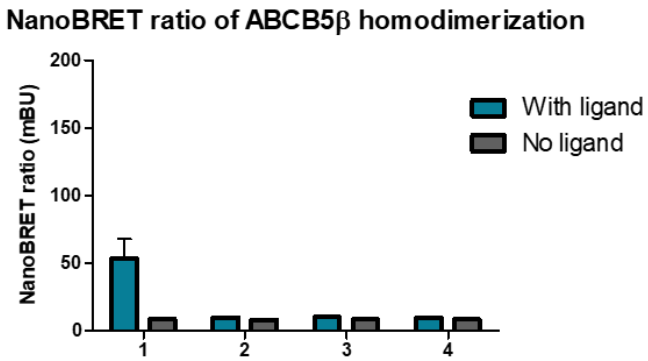

Mean corrected ratio:

B5β Nano N – B5β Halo N: 45,2 mBU

B5β Nano N – B5β Halo C: 1,7 mBU

B5β Nano C – B5β Halo N: 1,56 mBU

B5β Nano C – B5β Halo C: 1,22 mBU

NanoBRET ratio (mBU)	With ligand			No ligand		
B6 Nano N – B6 Halo N	65	64	65	8	8	8
B6 Nano N – B6 Halo C	54	56	54	8	8	8
B6 Nano C – B6 Halo N	19	20	20	8	8	8
B6 Nano C – B6 Halo C	66	62	62	8	8	8
B6 Nano N – B6 Halo N	63	62	62	9	9	9
B6 Nano N – B6 Halo C	47	48	49	9	9	9
B6 Nano C – B6 Halo N	27	27	24	9	9	8
B6 Nano C – B6 Halo C	73	73	68	8	8	10
B6 Nano N – B6 Halo N	60	61	61	9	9	8
B6 Nano N – B6 Halo C	64	64	63	9	8	8
B6 Nano C – B6 Halo N	21	22	20	8	8	8
B6 Nano C – B6 Halo C	94	96	81	8	8	8

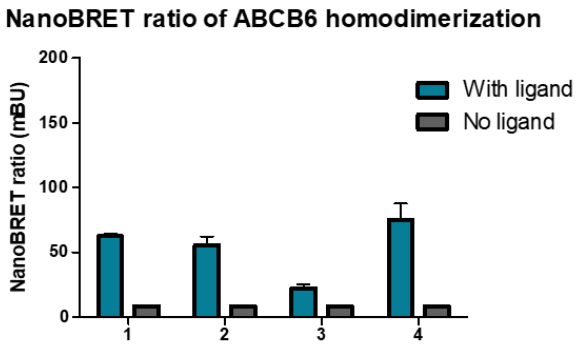

Mean corrected ratio:

B6 Nano N – B6 Halo N: 54,0 mBU

B6 Nano N – B6 Halo C: 47,0 mBU

B6 Nano C – B6 Halo N: 14,0 mBU

B6 Nano C – B6 Halo C: 66,8 mBU

NanoBRET ratio (mBU)	With ligand			No ligand		
B9 Nano N – B9 Halo N	71	73	69	9	9	9
B9 Nano N – B9 Halo C	100	90	85	9	9	9
B9 Nano C – B9 Halo N	106	97	93	8	8	9
B9 Nano C – B9 Halo C	124	135	119	8	9	8
B9 Nano N – B9 Halo N	79	80	90	10	9	8
B9 Nano N – B9 Halo C	60	60	64	9	9	8
B9 Nano C – B9 Halo N	56	57	59	8	8	8
B9 Nano C – B9 Halo C	104	107	100	8	8	7
B9 Nano N – B9 Halo N	67	69	72	9	9	8
B9 Nano N – B9 Halo C	63	64	63	9	9	9
B9 Nano C – B9 Halo N	67	67	58	8	8	7
B9 Nano C – B9 Halo C	129	123	114	8	8	8

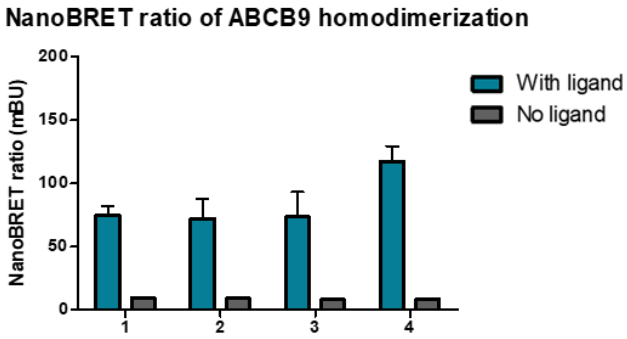

Mean corrected ratio:

B9 Nano N – B9 Halo N: 65,5 mBU

B9 Nano N – B9 Halo C: 63,2 mBU

B9 Nano C – B9 Halo N: 65,3 mBU

B9 Nano C – B9 Halo C: 109,2 mBU

Annex 7: ABCB5β, ABCB6 and ABCB9 hetero- and homodimerization dilution assay

(/ means that no ratio was calculable because of too low donor or acceptor emission)

B5β Nano N – B6 Halo N

	Mean NanoBRET ratio	Mean corrected ratio		Mean NanoBRET ratio	Mean corrected ratio
Ratio 1:1	82,3	74,3		89	80,3
Ratio 1:10	81,7	74		91	83
Ratio 1:100	99,7	/		110,3	/
Ratio 1:1000	135	/		100	/

B5β Nano N – B9 Halo N

	Mean NanoBRET ratio	Mean corrected ratio		Mean NanoBRET ratio	Mean corrected ratio
Ratio 1:1	78	69,3		84,7	76,7
Ratio 1:10	77,3	69,6		86,3	78,6
Ratio 1:100	75,7	67,7		74,7	67,7
Ratio 1:1000	74,7	/		/	/

B6 Nano N – B9 Halo N

	Mean NanoBRET ratio	Mean corrected ratio		Mean NanoBRET ratio	Mean corrected ratio
Ratio 1:1	96,3	87,6		97,7	88,7
Ratio 1:10	98	89,7		90	82
Ratio 1:100	99	90		98,3	86
Ratio 1:1000	95	/		121,3	/

B5β Nano N – B5β Halo N

	Mean NanoBRET ratio	Mean corrected ratio		Mean NanoBRET ratio	Mean corrected ratio
Ratio 1:1	48	39,3		54,7	47
Ratio 1:10	50	42		58,3	49,6
Ratio 1:100	/	/		/	/
Ratio 1:1000	/	/		/	/

B6 Nano C – B6 Halo C

	Mean NanoBRET ratio	Mean corrected ratio		Mean NanoBRET ratio	Mean corrected ratio
Ratio 1:1	50,3	42,3		55,7	47,7
Ratio 1:10	136,7	128		163,7	155,7
Ratio 1:100	212	204		205,7	198
Ratio 1:1000	204,7	196		201,3	192,6

B9 Nano C – B9 Halo C

	Mean NanoBRET ratio	Mean corrected ratio		Mean NanoBRET ratio	Mean corrected ratio
Ratio 1:1	54,7	46		57,3	49,3
Ratio 1:10	156,7	148,7		114	106,3
Ratio 1:100	156	148,3		153,3	145,6
Ratio 1:1000	148,7	139,2		121,7	114,7

Annex 8: ABCB5β homodimer donor saturation assay concentrations

NanoLuc DNA concentration (µg)	HaloTag DNA concentration (µg)	Ratio
0,20	3,554	177,7
0,20	2,369	118,5
0,20	1,580	79
0,20	1,053	52,65
0,20	0,702	35,1
0,20	0,468	23,4
0,20	0,312	15,6
0,20	0,208	10,4